AD-A169 580 GROUND RESPONSE IN ALLUVIAL BASINS DUE TO SEISMIC DISTURBANCES(U) COLUMBIA UNIV NEW YORK J T KUO ET AL. AUG 83 SCIENTIFIC-2 AFGL-TR-84-0104 F19628-81-K-0012 1/1

UNCLASSIFIED F/G 8/11 NL

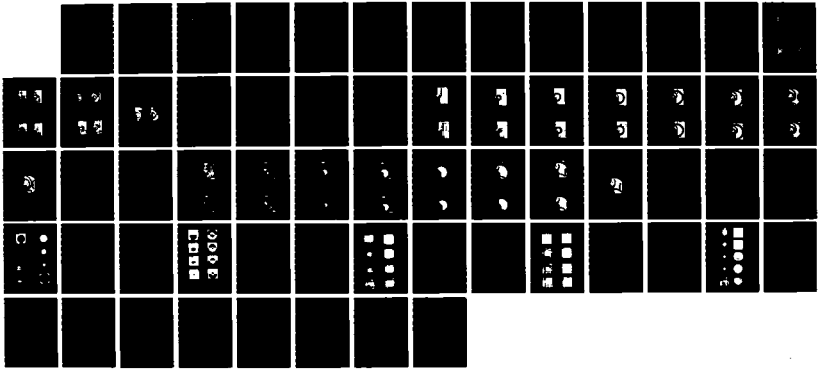

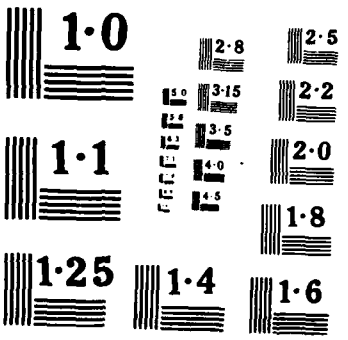
1·0
1·1
1·25
1·4
1·6
1·8
2·0
2·2
2·5
2·8
3·15
3·5
4·0
4·5
5·0

(12)

AFGL-TR-84-0104

GROUND RESPONSE IN ALLUVIAL BASINS DUE TO SEISMIC DISTURBANCES

John T. Kuo
Yu-Chiung Teng

Columbia University
New York, NY 10027

August 1983

Scientific Report No. 2

Approved for public release
distribution unlimited

AIR FORCE GEOPHYSICS LABORATORY
AIR FORCE SYSTEMS COMMAND
UNITED STATES AIR FORCE
HANSCOM AFB, MASSACHUSETTS 01731

CONTRACTOR REPORTS

This technical report has been reviewed and is approved for publication.

JAMES C. BATTIS
Contract Manager

HENRY A. OSSING
Chief, Solid Earth Geophysics Branch

FOR THE COMMANDER

DONALD H. ECKHARDT
Director
Earth Sciences Division

This report has been reviewed by the ESD Public Affairs Office (PA) and is releasable to the National Technical Information Service (NTIS).

Qualified requesters may obtain additional copies from the Defense Technical Information Center. All others should apply to the National Technical Information Service.

If your address has changed, or if you wish to be removed from the mailing list, or if the addressee is no longer employed by your organization, please notify AFGL/DAA, Hanscom AFB, MA 01731-5000. This will assist us in maintaining a current mailing list.

Do not return copies of this report unless contractual obligations or notices on a specific document requires that it be returned.

REPORT DOCUMENTATION PAGE

1a. REPORT SECURITY CLASSIFICATION: Unclassified	1b. RESTRICTIVE MARKINGS
2a. SECURITY CLASSIFICATION AUTHORITY	3. DISTRIBUTION/AVAILABILITY OF REPORT: Approved for public release; distribution unlimited
2b. DECLASSIFICATION/DOWNGRADING SCHEDULE	
4. PERFORMING ORGANIZATION REPORT NUMBER(S)	5. MONITORING ORGANIZATION REPORT NUMBER(S): AFGL-TR-84-0104
6a. NAME OF PERFORMING ORGANIZATION: Columbia University; 6b. OFFICE SYMBOL (If applicable)	7a. NAME OF MONITORING ORGANIZATION: Air Force Geophysics Laboratory
6c. ADDRESS (City, State and ZIP Code): New York, NY 10027	7b. ADDRESS (City, State and ZIP Code): Hanscom AFB, Massachusetts 01731
8a. NAME OF FUNDING/SPONSORING ORGANIZATION; 8b. OFFICE SYMBOL (If applicable): LWH	9. PROCUREMENT INSTRUMENT IDENTIFICATION NUMBER: F19628-81-K-0012
8c. ADDRESS (City, State and ZIP Code)	10. SOURCE OF FUNDING NOS.

PROGRAM ELEMENT NO.	PROJECT NO.	TASK NO.	WORK UNIT NO.
61102F	2309	G2	AH

11. TITLE (Include Security Classification): Ground Response in Alluvial Basins Due to Seismic Disturbances

12. PERSONAL AUTHOR(S): John T. Kuo and Yu-Chiung Teng

13a. TYPE OF REPORT	13b. TIME COVERED	14. DATE OF REPORT (Yr., Mo., Day)	15. PAGE COUNT
Sci Rpt No. 2	FROM _____ TO _____	1983 August	62

16. SUPPLEMENTARY NOTATION

17 COSATI CODES		
FIELD	GROUP	SUB. GR

18. SUBJECT TERMS (Continue on reverse if necessary and identify by block number): Finite element; Seismic wave; Propagation; Surface waves; Alluvial basins

19. ABSTRACT (Continue on reverse if necessary and identify by block number)

This summarizes the second year's accomplishments under Contract F19628-81-K-0012. Our scientific accomplishments include studying three finite element models for SH waves or elastic (P and SV) waves with display of snapshots, and studying finite element source mechanism, and modifying the two-dimensional finite element computer codes for SH waves and elastic waves. Five different types of source, including concentrated coupled line source and non-directional line source for elastic waves, are considered. The 2-CST formulation and nodal-point-oriented technique have been introduced to the computer codes.

20. DISTRIBUTION/AVAILABILITY OF ABSTRACT	21. ABSTRACT SECURITY CLASSIFICATION
UNCLASSIFIED/UNLIMITED ☐ SAME AS RPT ☐ DTIC USERS ☐	Unclassified

22a. NAME OF RESPONSIBLE INDIVIDUAL	22b. TELEPHONE NUMBER (Include Area Code)	22c. OFFICE SYMBOL
James Battis	(617) 377-3767	AFGL/LWH

DD FORM 1473, 83 APR — EDITION OF 1 JAN 73 IS OBSOLETE

TABLE OF CONTENTS

INTRODUCTION

In the second year of Contract F19628-81-K-ØØ12, "Ground Response Alluvial Basins Due to Seismic Disturbances", from March 26, 1982, our research emphasis has been in the following four areas:

I. Solving the finite element basin models for elastic (P and S) waves, models considered are relatively more complex than what we studied in the period of the first year of the Contract.

II. Studying the finite element source mechanism for the cases:

(A) One Degree of Freedom SH-wave Problem with :

(i) concentrated line source,

(ii) concentrated coupled line source.

(B) Two Degrees of Freedom Elastic Wave Problems with:

(i) directional concentrated line source,

(ii) concentrated coupled line source.

(iii) non-directional line source,

III. Modifying and improving our two-dimensional finite element codes for the cases of elastic and SH- waves by:

(A) replaceing the 4CST(Four Constant Strain Triangles) algorithm by the Averaging 2CST algorithm,

(B) replacing the element-oriented approach by the nodal-point-oriented approach,

(C) changing the structure of the global assemblage

system.

IV. Implementing the two-dimensional finite element codes with a snapshots plotting software.

SCIENTIFIC ACCOMPLISHMENTS

I. Finite Element Modeling of Preliminary Basins

(A) Partial Basins with Display of Synthetic Seismogram

As a continuation, we have studied two preliminary basin models as shown in Figures 1 and 2 for the case of elastic (P and S) waves. The results for the corresponding SH-wave case have been reported in the Scientific Report No. 1 (Kuo and Teng, 1982). In Figure 1 (Model 3-A in the Scientific Report No. 1), a homogeneous material with v_p = 5,000 m/sec, v_s = 2,900 m/sec, ρ = 2.67 gm/cm^3, is excited by a vertical function $F_o(t)$ as shown in Figure 7-B at Point S on the free surface of the deeper basin DC, while the receivers are located on the free surface of the shallower basin in the region BC. In Figure 2 (Model 3-B in the Scientific Repeort No. 1, Kuo and Teng, 1982), a vertical source is located in the shallower basin, while the receivers are in the deeper basin. Again, the forcing function is the first derivative of a Gaussian function with its center frequency $f_c \sim$ 2.7 Hz. Figures 3 and 4 are the results of the displacement components along plane ABC in both models respectively.

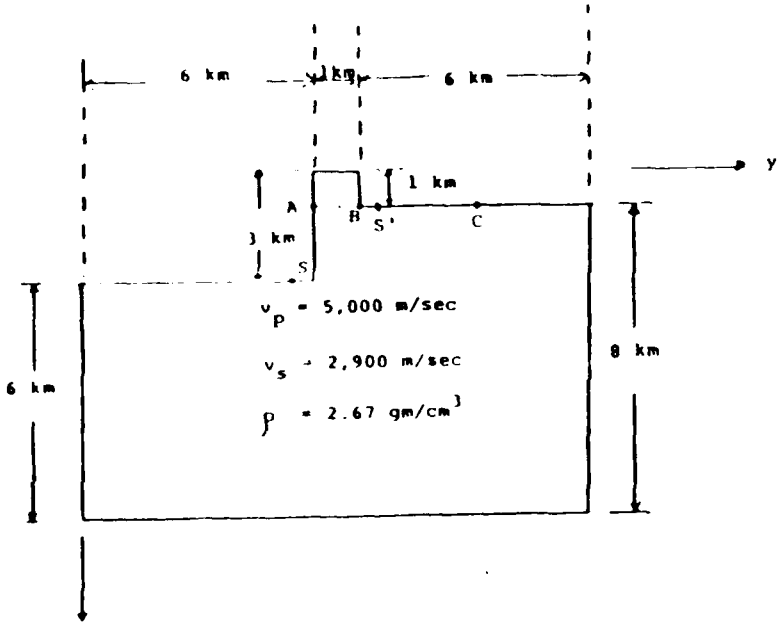

Figure 1 . Preliminary Basin Model 3-A for Elastic Waves.

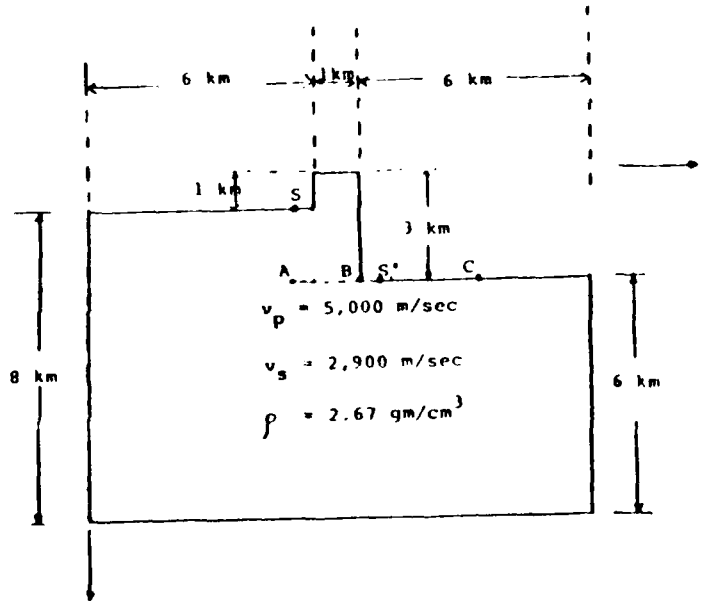

Figure 2. Preliminary Basin Model 3-B for Elastic Waves.

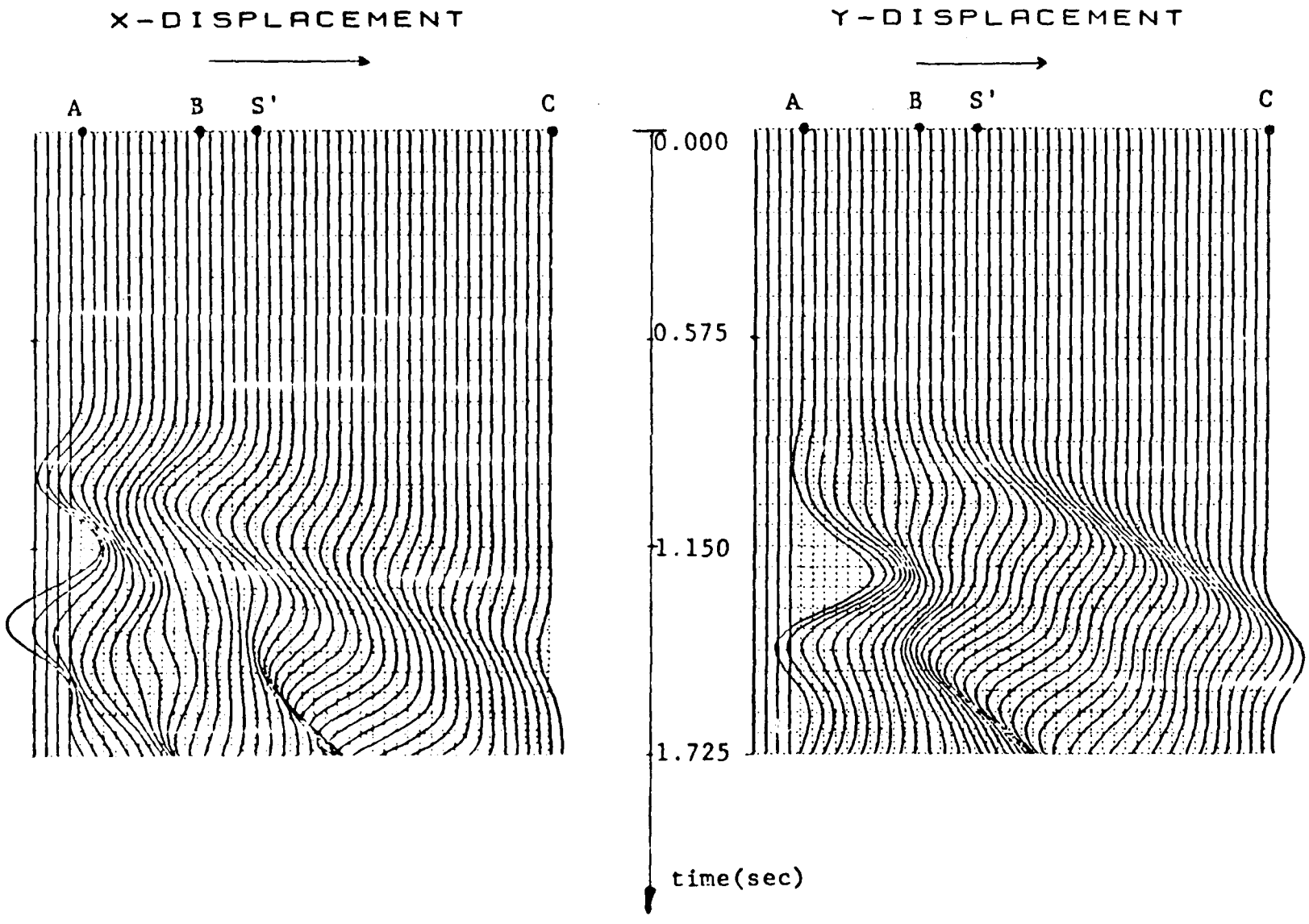

Figure 3. Synthetic Seismogram Along ABC of Model 3-A.

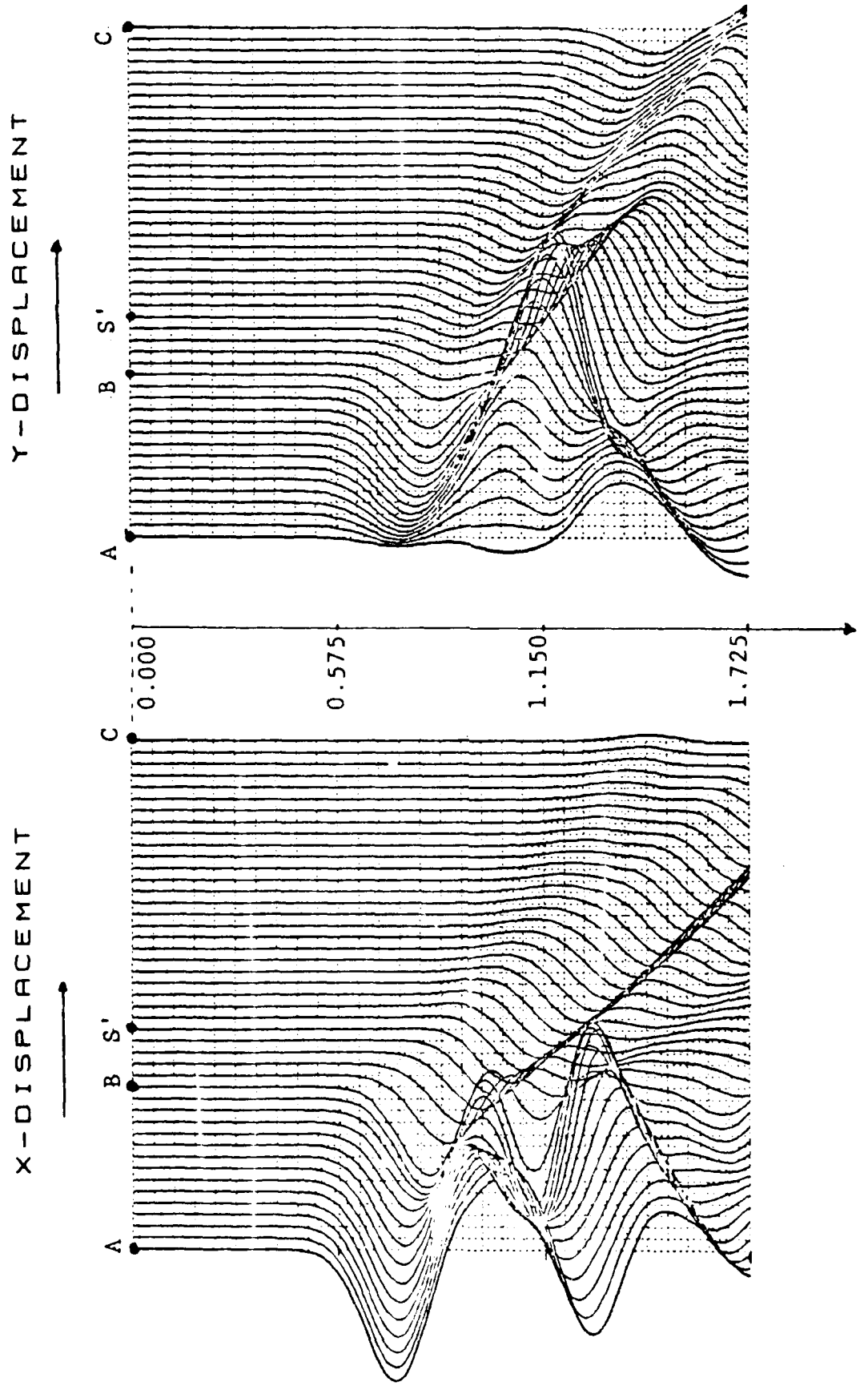

Figure 4. Synthetic Seismogram Along ABC of Model 3-B.

(B) Partial Basins with Display of Snapshots

In order to obtain clearer display of the results for the basin modeling, an Aldridge Laboratory computer code for snapshots has been implemented to our finite elemenet computer codes. The display of snapshots provides a technique whereby the time history of the interaction can be visualized and the resulting wave shapes, direction of propagation and nature of mode conversion can be identified. For demonstration, the snapshots have been made for the following three cases:

Case I: Model 3-A for Elastic Waves

Figures 5-A to 5-G are snapshots of the synthetic wavefield at Ø.3 sec intervals. Vertical and horizontal displacement components are given separately. Each snapshot is independently scaled and the amplitudes magnified 1Ø times. Black is positive displacement and white is negative displacement. Diffracted waves at the square corners are clearly identified after Ø.9 sec.

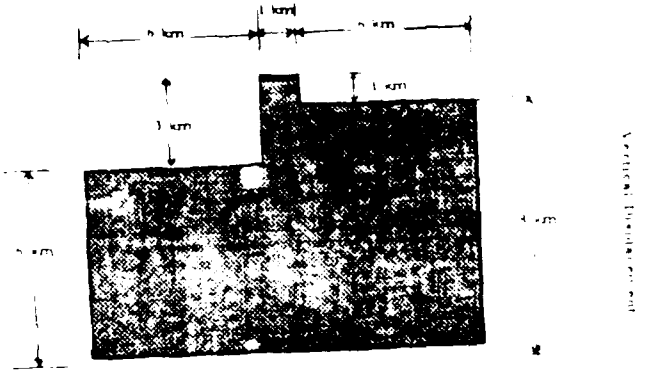

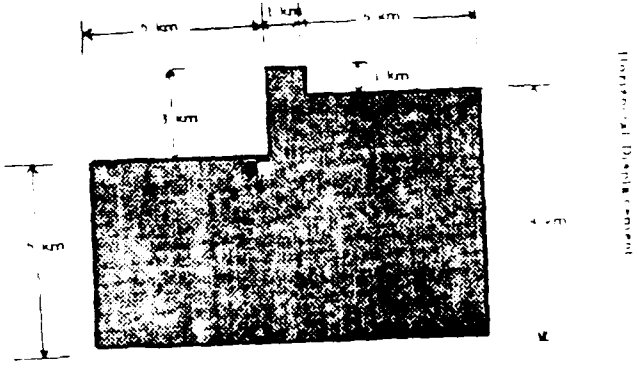

v_p = 5,000 m/sec

v_s = 2,300 m/sec, ρ = 2.67 gm/cm^3

Figure 5-A. A Snapshot View of Wave Pattern at 0.3 sec after the Detonation of the Source.

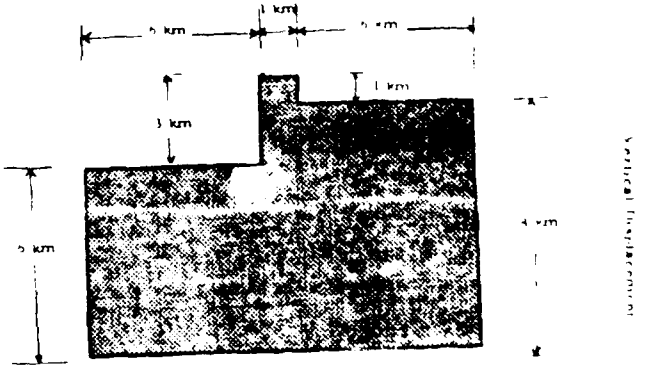

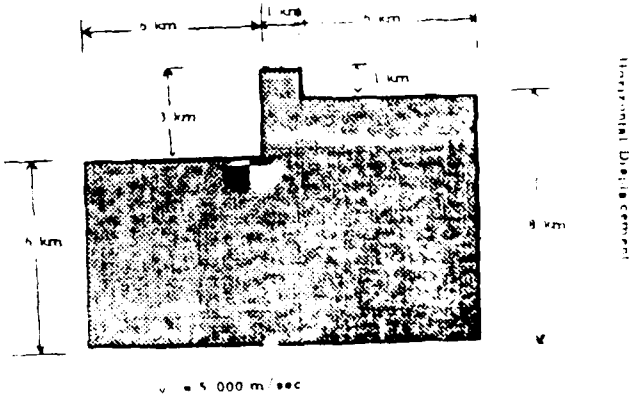

v_p = 5,000 m/sec

v_s = 2,300 m/sec, ρ = 2.67 gm/cm^3

Figure 5-B. A Snapshot View of Wave Pattern at 0.6 sec after the Detonation of the Source.

Figure 5-C. A Snapshot View of Wave Pattern at 0.9 sec after the Detonation of the Source.

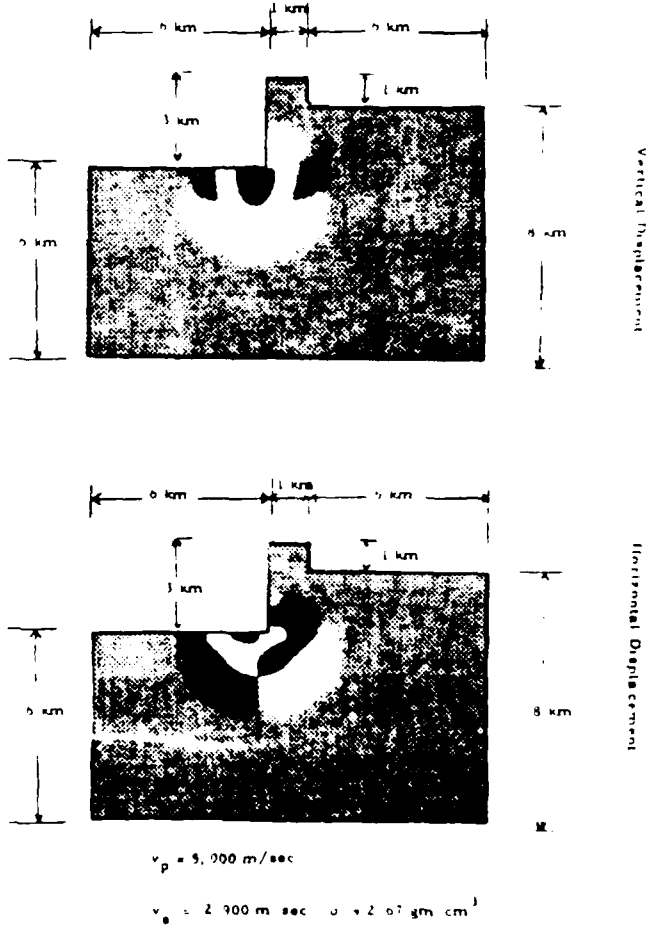

Figure 5-D. A Snapshot View of Wave Pattern at 1.2 sec after the Detonation of the Source.

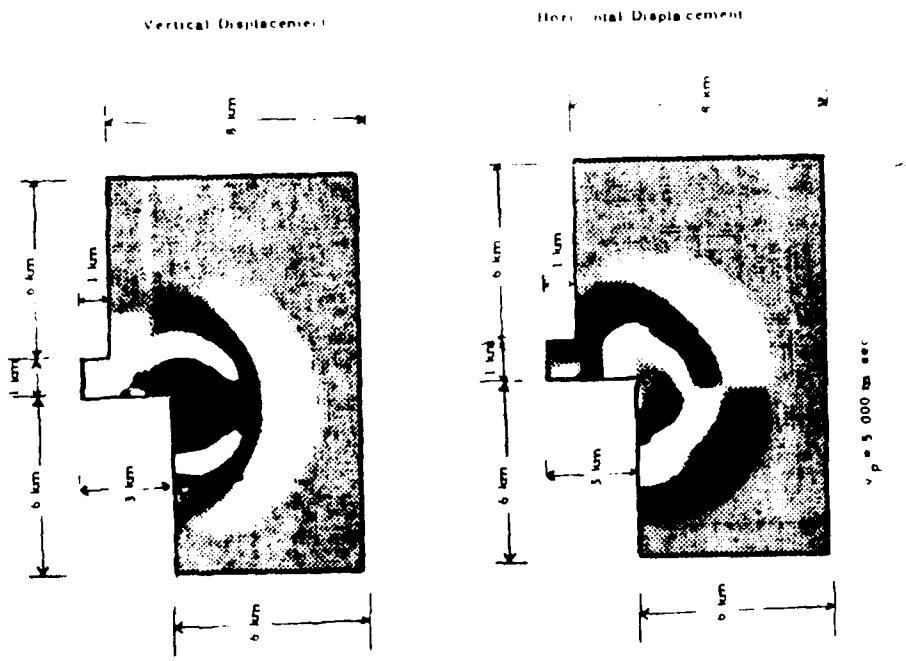

Figure 5-F. A Snapshot View of Wave Pattern at 1.8 secs after the Detonation of the Source.

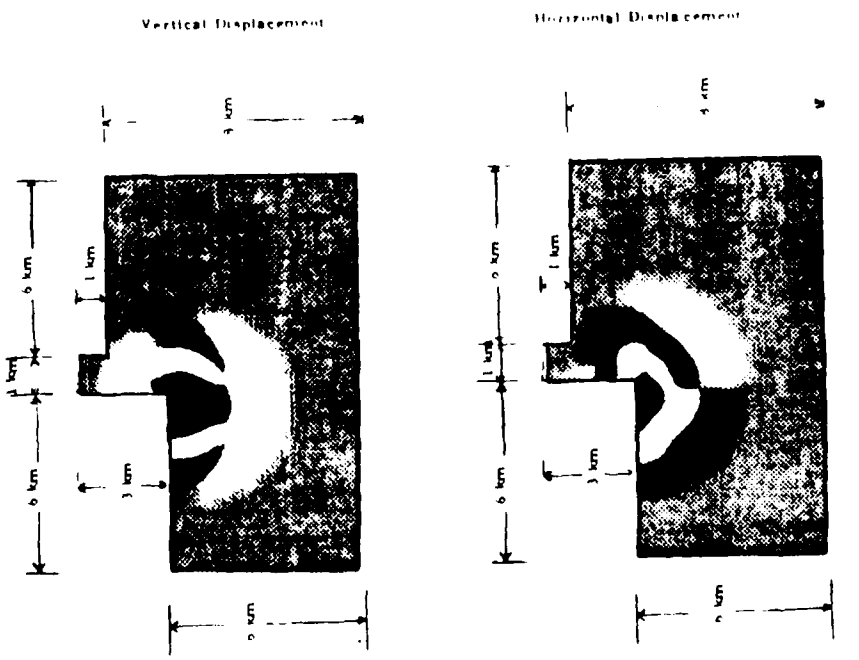

Figure 5-E. A Snapshot View of Wave Pattern at 1.5 secs after the Detonation of the Source.

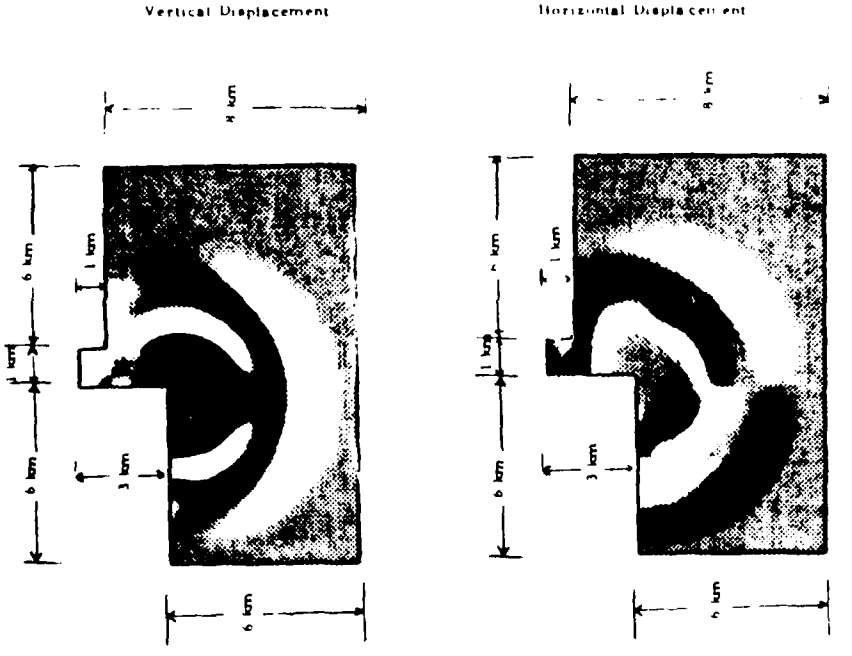

Figure 5-G. A Snapshot View of Wave Pattern at 2.1 secs after the Detonation of the Source.

Case 2: Model 3-A for SH-Wave

In Figure 6, a SH-wave source $F_1(t)$ is located at the corner S of the lower basin. The source function $F_1(t)$ is shown in Figure 7-A. Figures 8-A to 8-O are the snapshots of the synthetic wavefield at Ø.2 sec intervals. In this simple one-degree-of-freedom problem, the reflections from the free surfaces and the diffractions from the corners can be clearly identified. Figures 8-M to 8-O, we observed that the wavefields are contaminated by the undesired reflections from the side and the bottom boundaries.

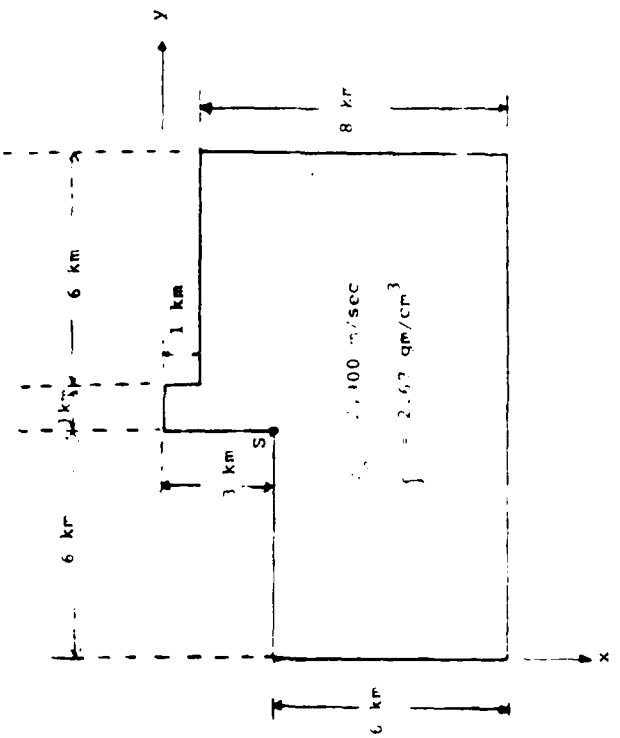

Figure 6. Preliminary Basin Model 3-A.

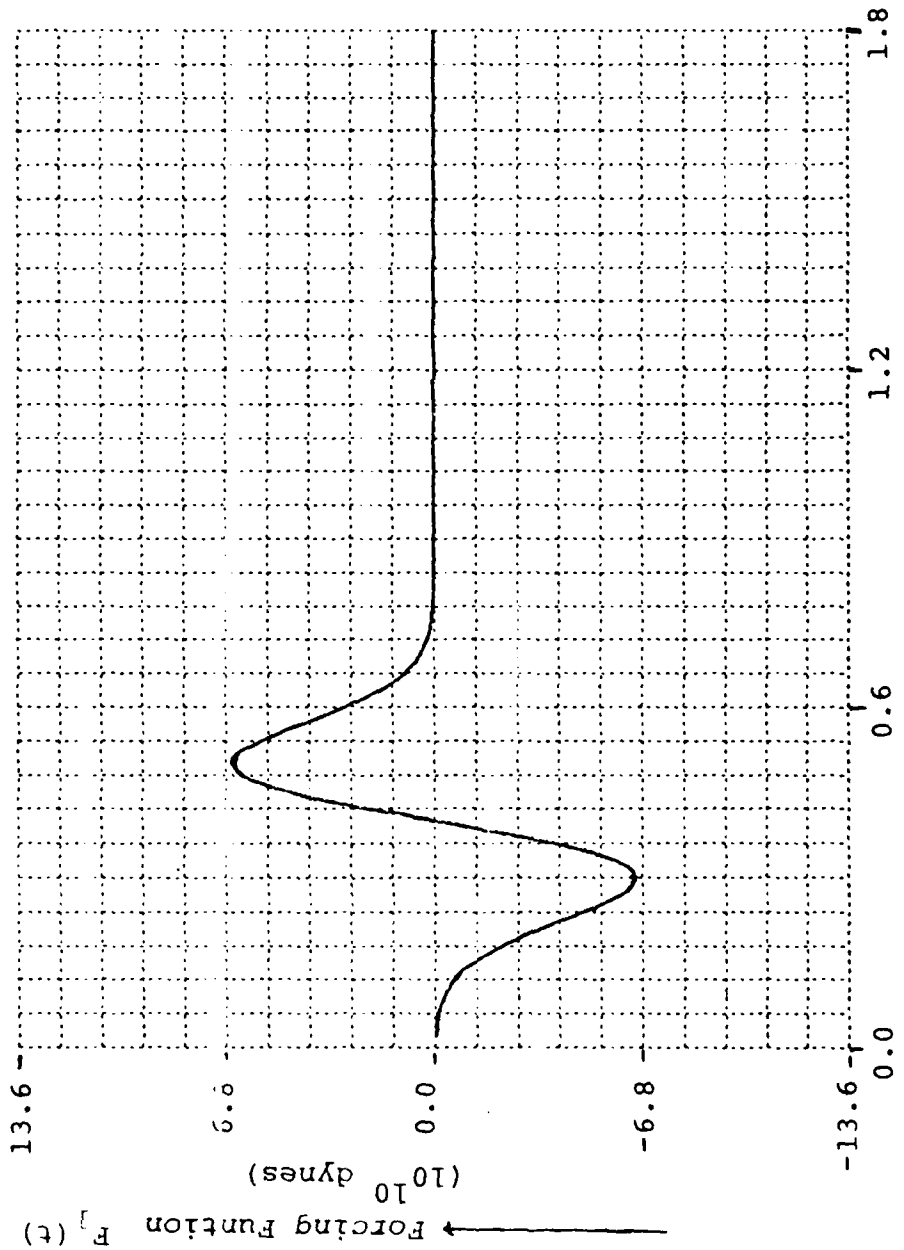

Figure 7-A. Source Function for SH-Wave Cases.

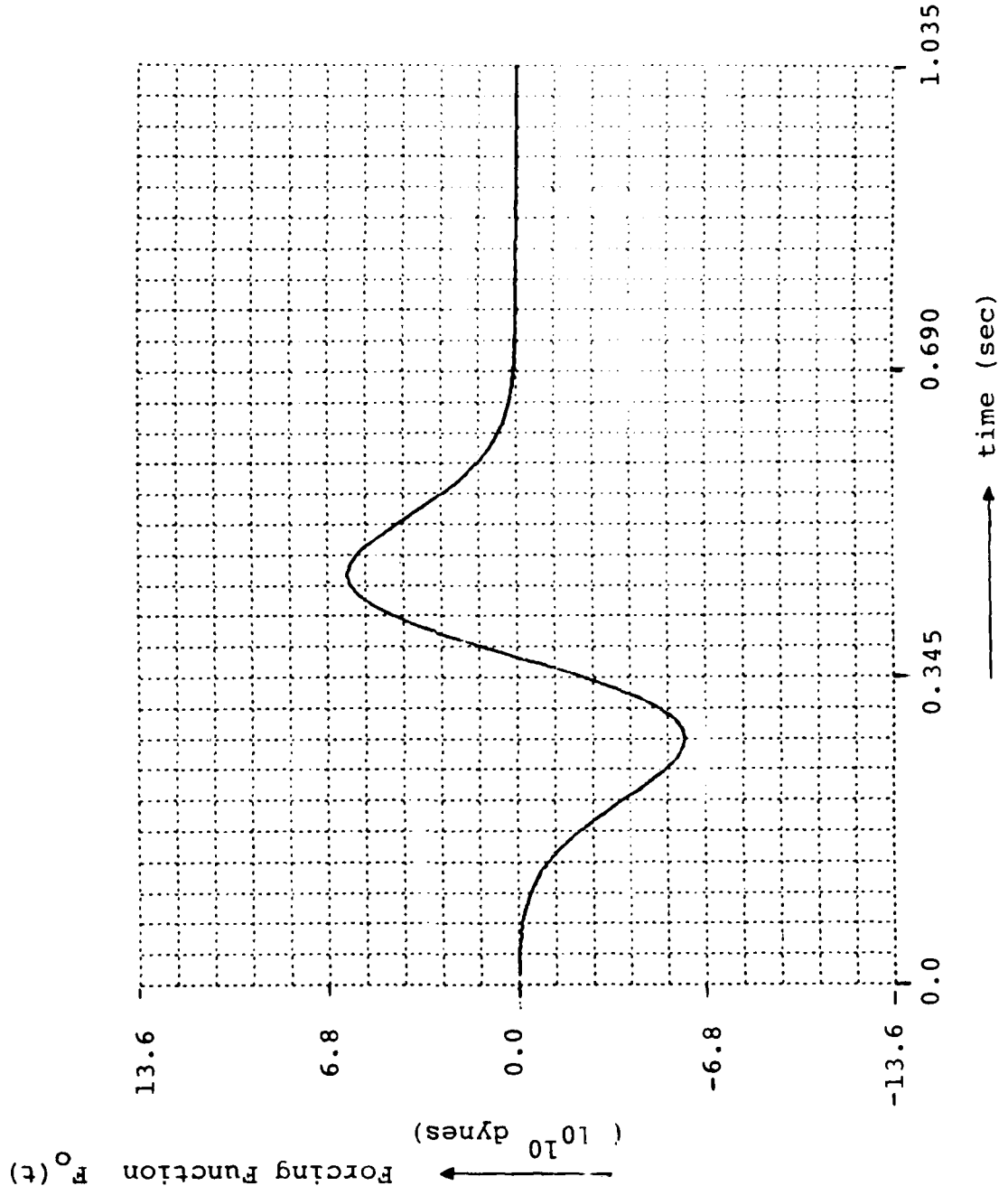

Figure 7-B. Source Function for Elastic Cases.

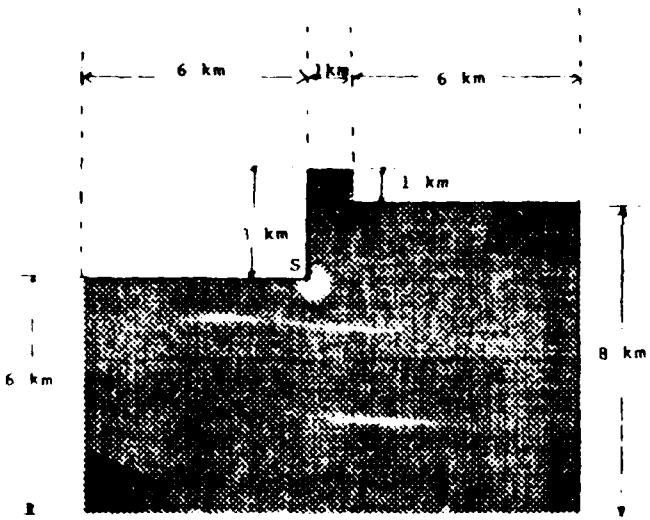

Figure 8-A . A Snapshot View of Wave Pattern at 0.2 sec after the Detonation of the Source.

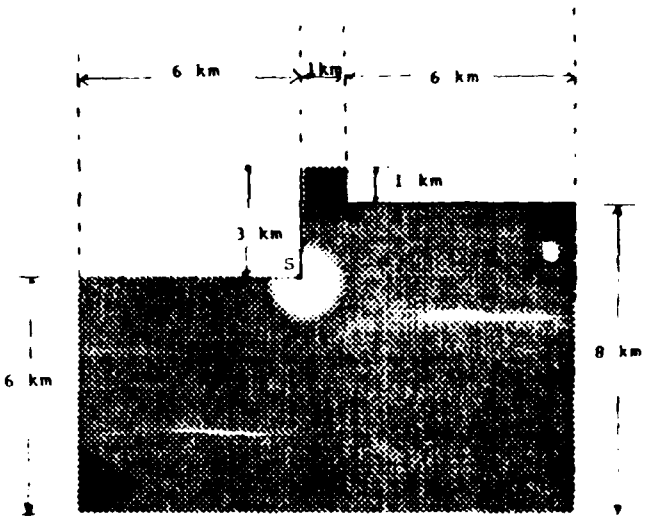

Figure 8-B . A Snapshot View of Wave Pattern at 0.4 sec after the Detonation of the Source.

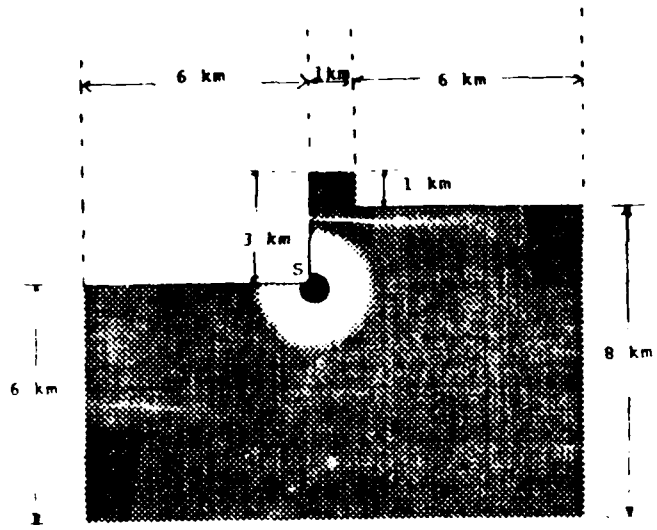

Figure 8-C . A Snapshot View of Wave Pattern at 0.6 sec after the Detonation of the Source.

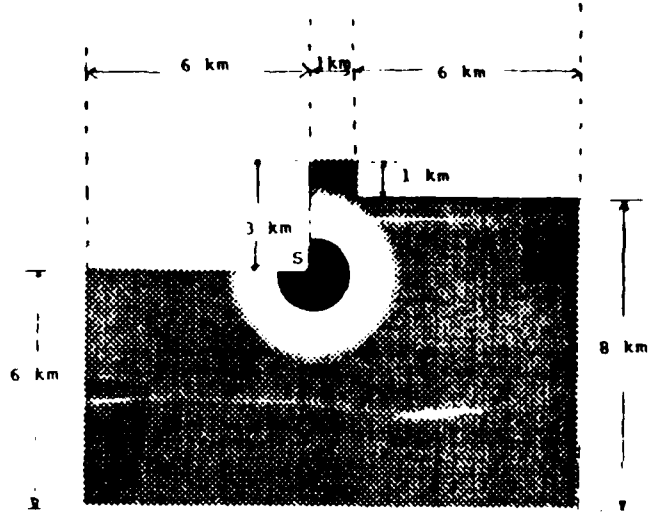

Figure 8-D . A Snapshot View of Wave Pattern at 0.8 sec after the Detonation of the Source.

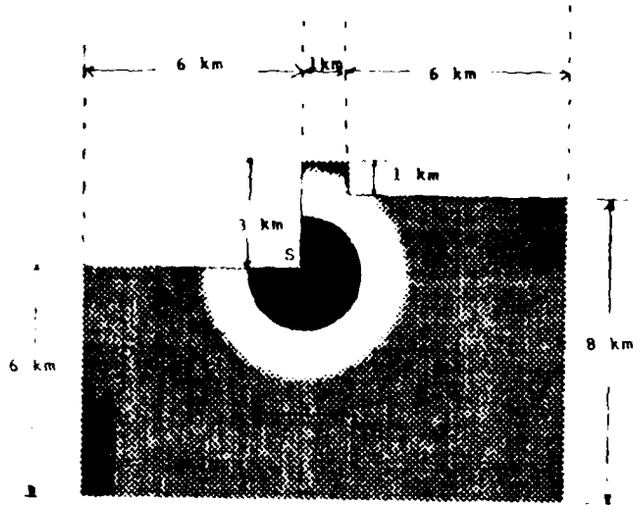

Figure 8-1 . A Snapshot View of Wave Pattern at 1.0 sec after the Detonation of the Source.

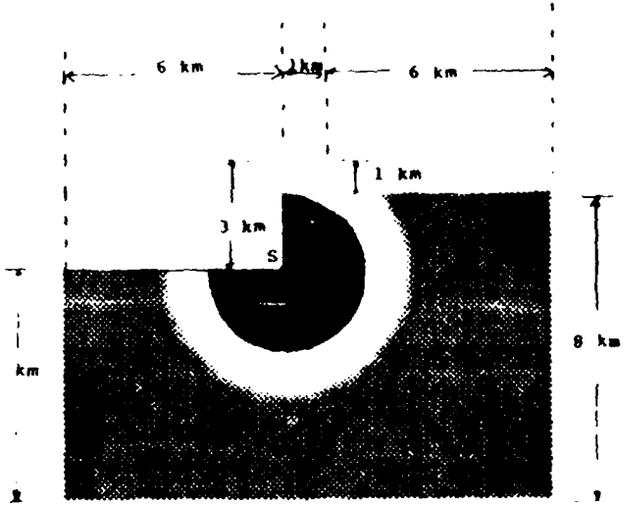

Figure 8-2 . A Snapshot View of Wave Pattern at 1.2 sec after the Detonation of the Source.

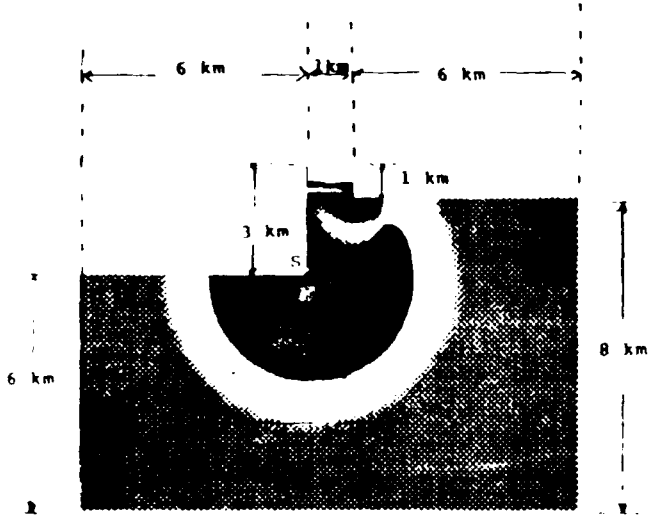

Figure 8-G . A Snapshot View of Wave Pattern at 1.4 sec after the Detonation of the Source.

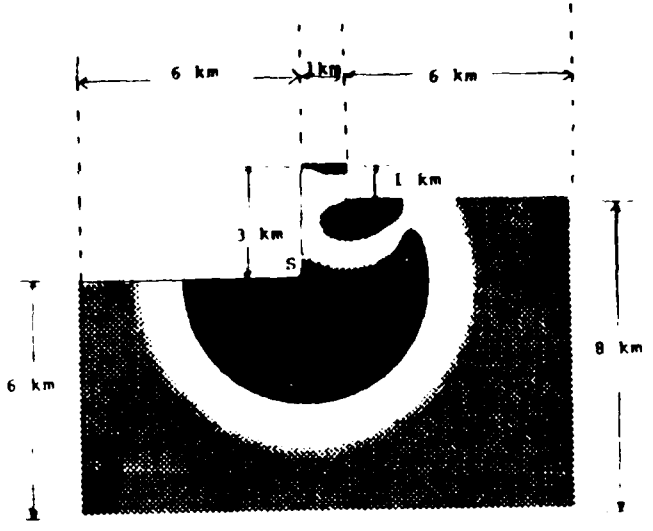

Figure 8-H . A Snapshot View of Wave Pattern at 1.6 sec after the Detonation of the Source.

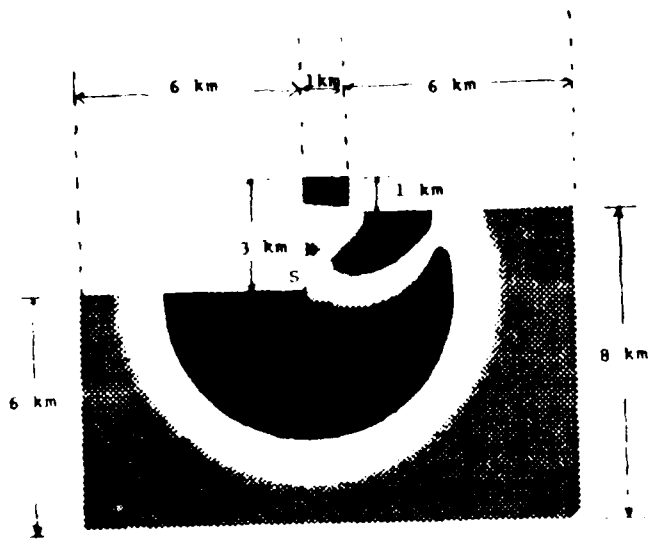

Figure 8-1 . A Snapshot View of Wave Pattern at 1.8 sec after the Detonation of the Source.

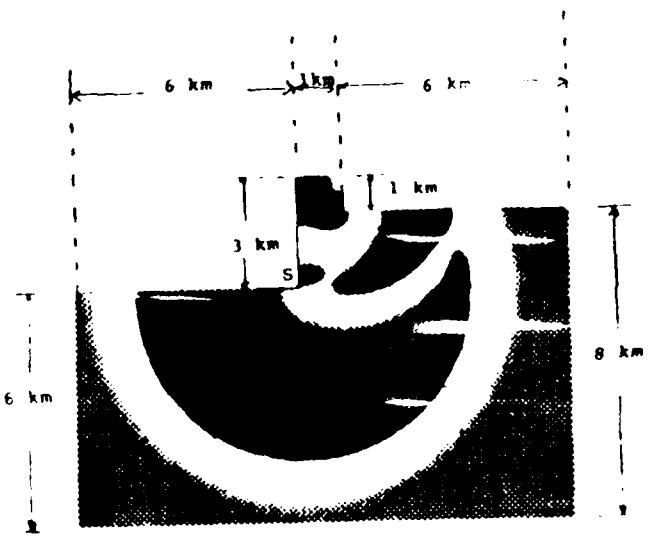

Figure 8-2 . A Snapshot View of Wave Pattern at 2.0 sec after the Detonation of the Source.

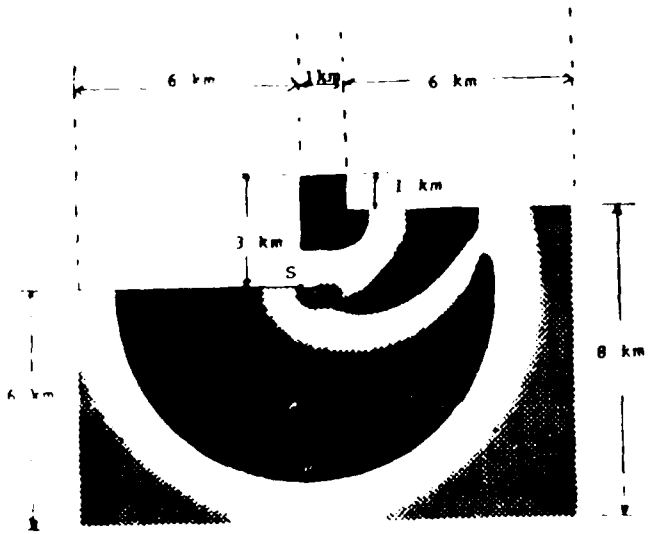

Figure 8.1. . A Snapshot View of Wave Pattern at 2.2 sec after the Detonation of the Source.

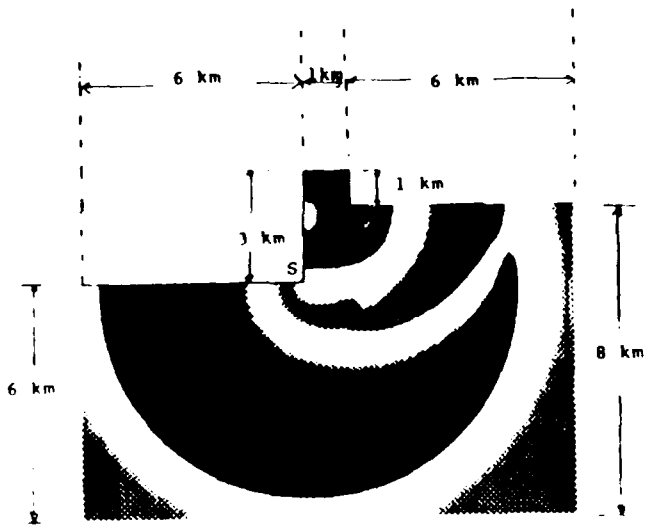

Figure 8.1. . A Snapshot View of Wave Pattern at 2.4 sec after the Detonation of the Source.

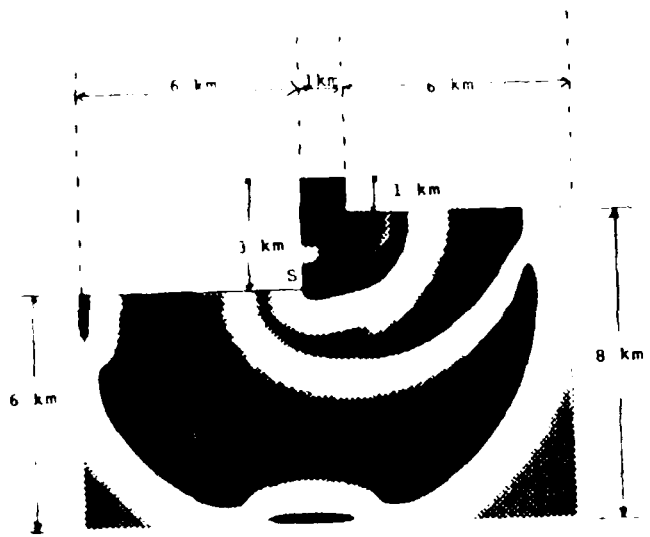

Figure 8-M . A Snapshot View of Wave Pattern at 2.6 sec after the Detonation of the Source.

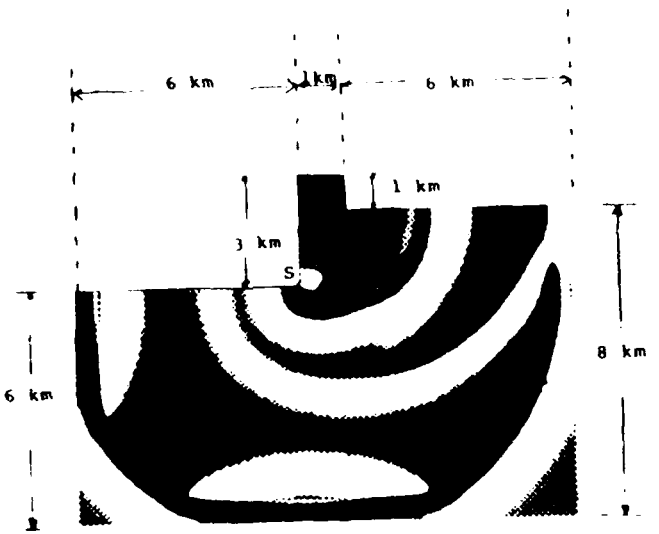

Figure 8-N . A Snapshot View of Wave Pattern at 2.8 sec after the Detonation of the Source.

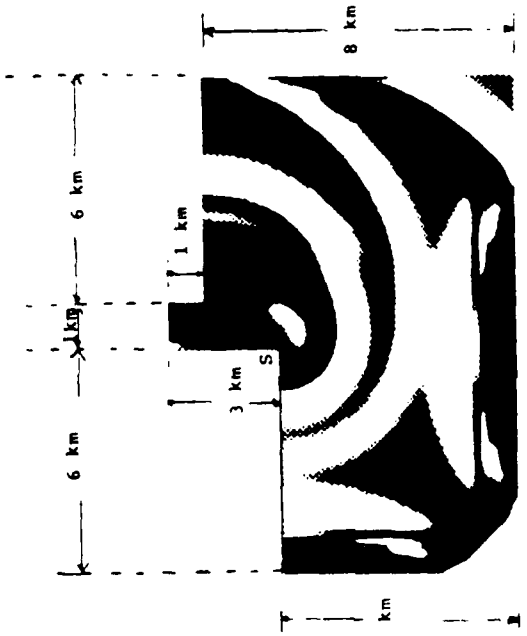

Figure 8-0 . A Snapshot View of Wave Pattern at 3.0 sec after the Detonation of the Source.

Case 3: Model 4 for SH-Wave

Figure 9 is the geometry of a preliminary basin model with an inclined slope of 45 . A SH-wave source function $F_1(t)$ (Figure 7-A) is located at the corner S . Figures 10-A to 10-O are the snapshots of the synthetic wavefield at 0.2 sec intervals. Two seconds after detonation of the source undesired reflections start. Comparing the results of this case with those of Case 2, a different phenomena can be seen in Figures 10-K to 10-O. In the neighborhood of the source location, the medium is quiescent 2.2 sec after detonation of the source. In Case 2, however, there is no such quiescent period. A reflection appears from the vertical portion of the free surface boundaries.

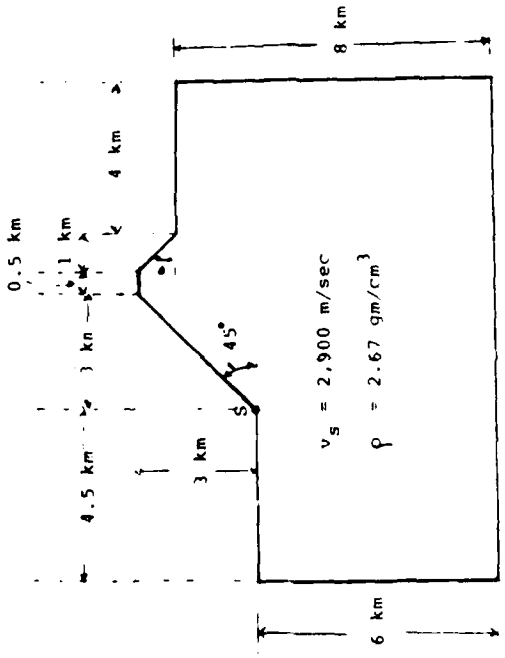

Figure 9. [illegible] Model 4.

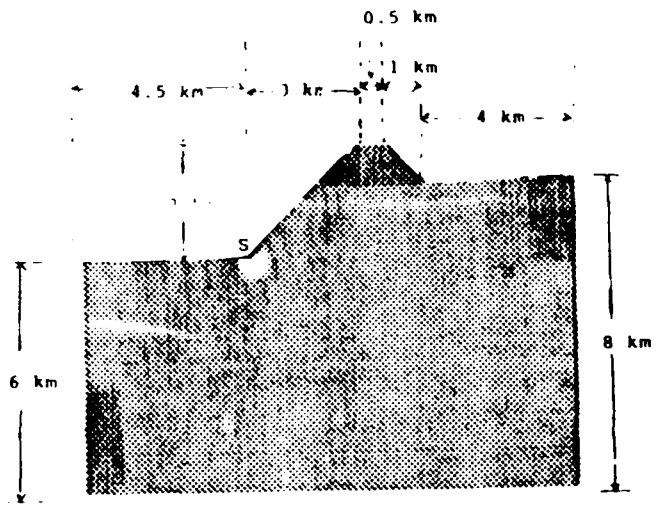

Figure 10-A . A Snapshot View of Wave Pattern at 0.2 sec after the Detonation of the Source.

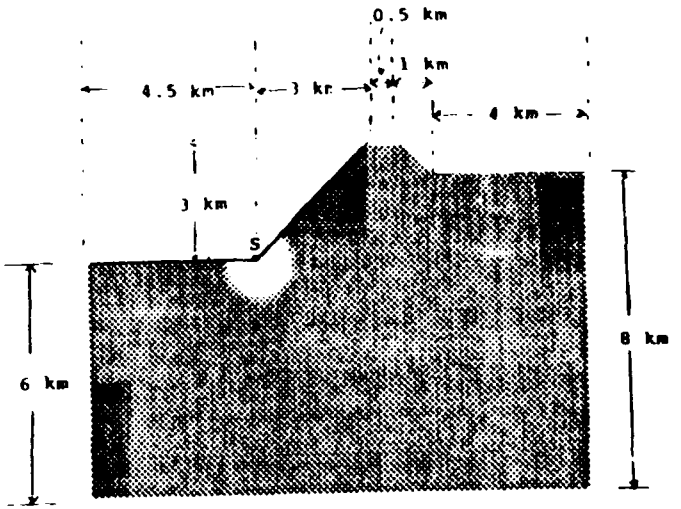

Figure 10-B . A Snapshot View of Wave Pattern at 0.4 sec after the Detonation of the Source.

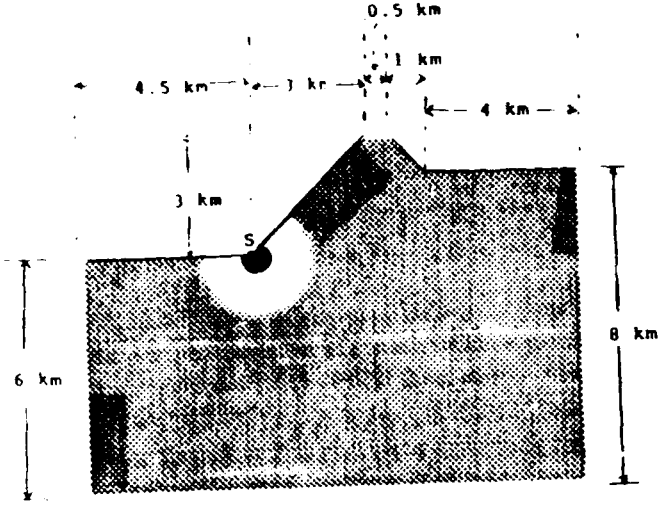

Figure 10-C . A Snapshot View of Wave Pattern at 0.6 sec after the Detonation of the Source.

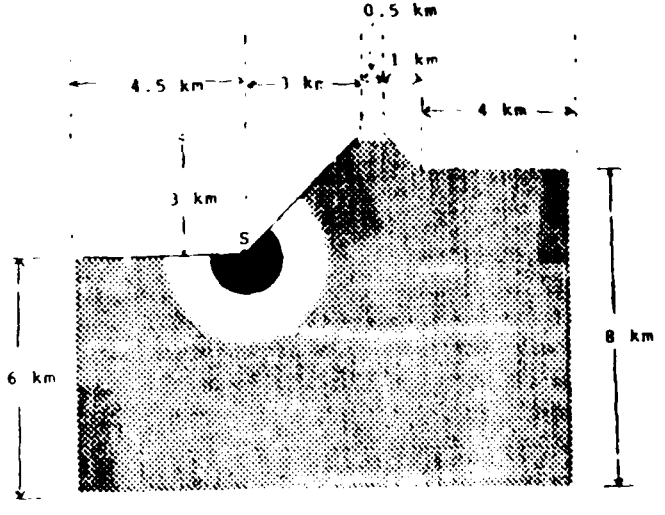

Figure 10-D . A Snapshot View of Wave Pattern at 0.8 sec after the Detonation of the Source.

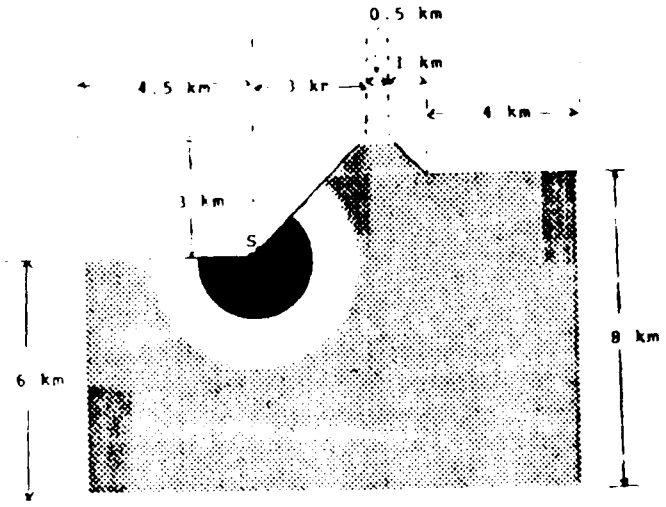

Figure 10-E . A Snapshot View of Wave Pattern at 1.0 sec after the Detonation of the Source.

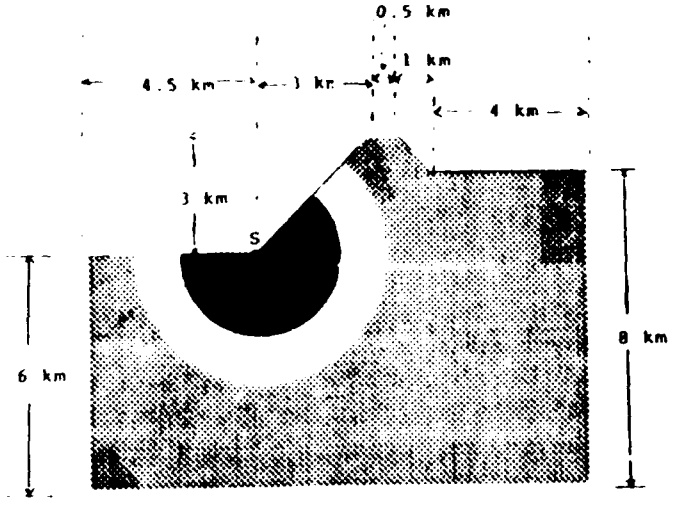

Figure 10-F . A Snapshot View of Wave Pattern at 1.2 sec after the Detonation of the Source.

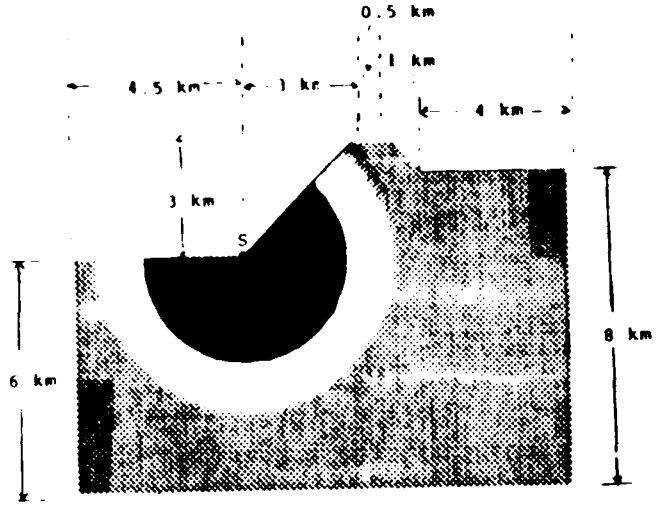

Figure 10-G . A Snapshot View of Wave Pattern at 1.4 sec after the Detonation of the Source.

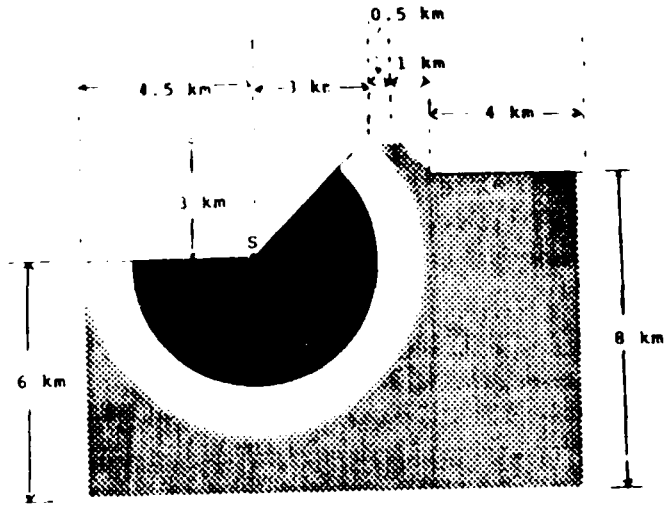

Figure 10-H . A Snapshot View of Wave Pattern at 1.6 sec after the Detonation of the Source.

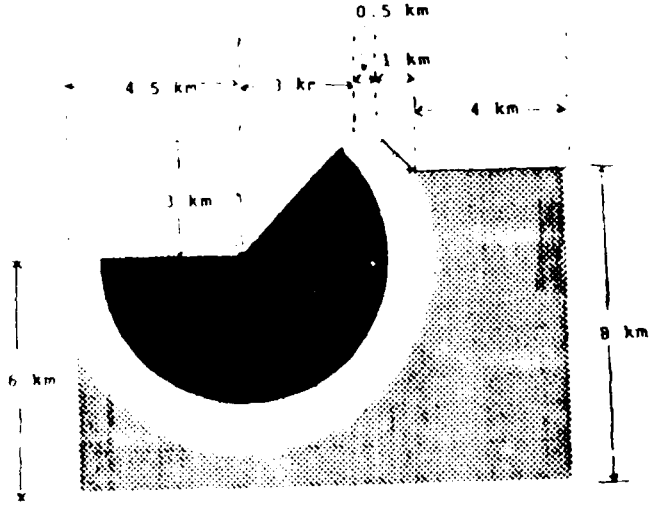

Figure 10-1. A Snapshot View of Wave Pattern at 1.8 sec after the Detonation of the Source.

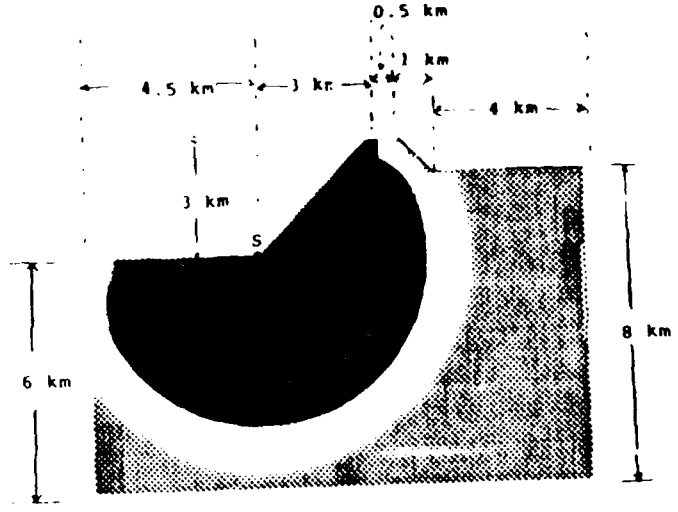

Figure 10-2. A Snapshot View of Wave Pattern at 2.0 sec after the Detonation of the Source.

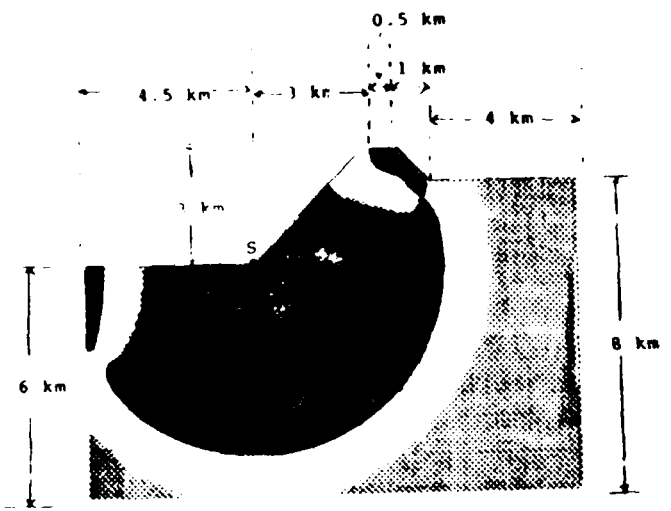

Figure 10-K . A Snapshot View of Wave Pattern at 2.2 sec after the Detonation of the Source.

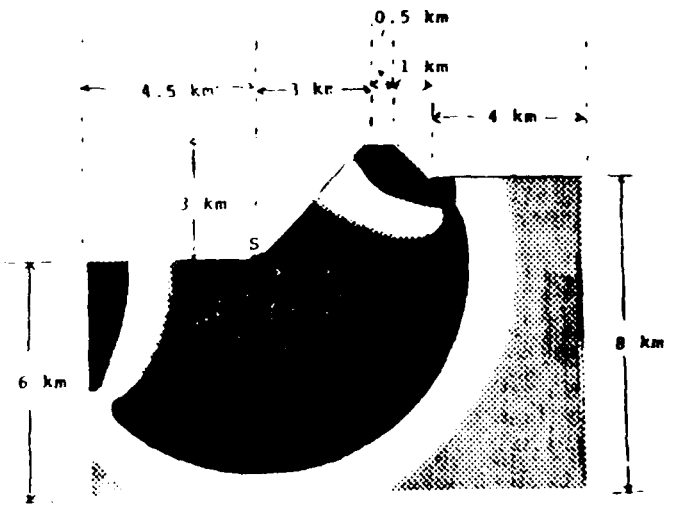

Figure 10-L . A Snapshot View of Wave Pattern at 2.4 sec after the Detonation of the Source.

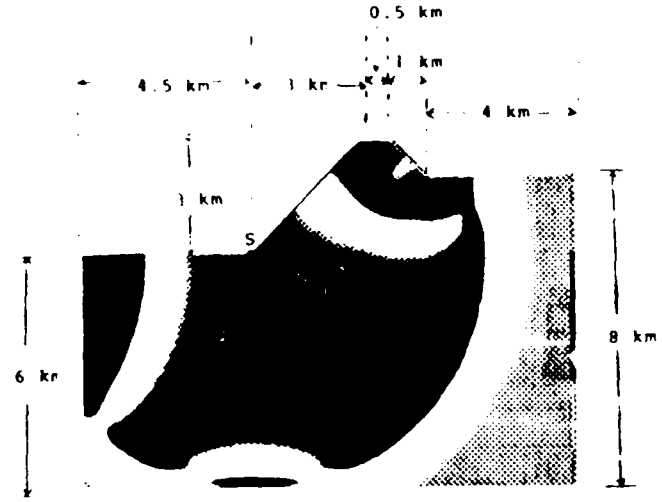

Figure 10-M . A Snapshot View of Wave Pattern at 2.6 sec after the Detonation of the Source.

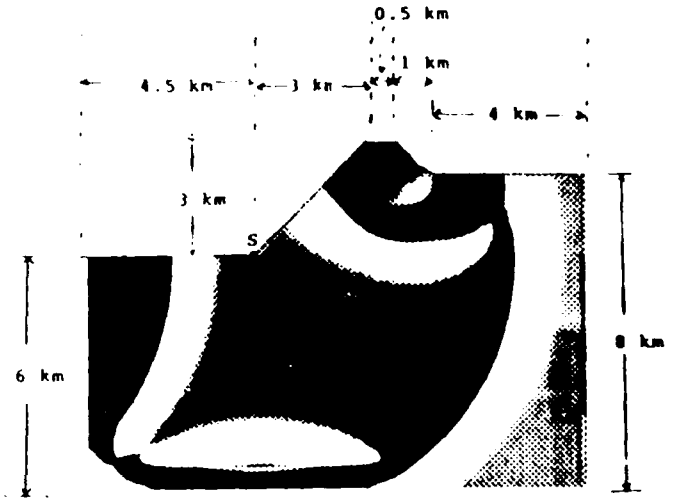

Figure 10-N . A Snapshot View of Wave Pattern at 2.8 sec after the Detonation of the Source.

Figure 10-6. A Snapshot View of Wave Pattern at 3.0 sec after the Detonation of the Source.

II. Finite element Source Mechanism

In finite element algorithms, the simulation of a non-directional line or point source, (the cylindrical source for two-dimensional problem, or the spherical source for three-dimensional problem), for the two- or three-degree-of-freedom elastic wave case has been a very challenging subject. The simplest or the most natural way to excite the elastic medium is to apply a directional forcing function to the structure. Likewise, for the one-degree-of-freedom problem, special effort is needed to simulate a couple source. In the Scientific Report No. 1 (Kuo and Teng, 1982) of the present Contract, we proposed to investigate systematically this subject by using a energy-sharing-nodal-points technique. During the past year, we have studied the two-dimensional source mechanism problems for the cases of SH-waves and elastic waves (both P and S) respectively. For the SH-wave case, two types of sources are considered: (i) concentrated line source, and (ii) concentrated coupled line source. For the elastic wave case, three types of sources are considered: (i) concentrated vertical (directional) line source, (ii) concentrated coupled line source, and (iii) concentrated non-directional line source.

Consider a two-dimensional whole space elastic medium, with v_p = 5,ØØØ m/sec, v_s = 2,9ØØ m/sec, ρ =2.67 gm/cm^3, Figure 11 shows the finite element mesh. In each dimension, 3Ø elements are used. Point S(Ø,Ø) is the location of the external source. Using this model, we studied the following cases:

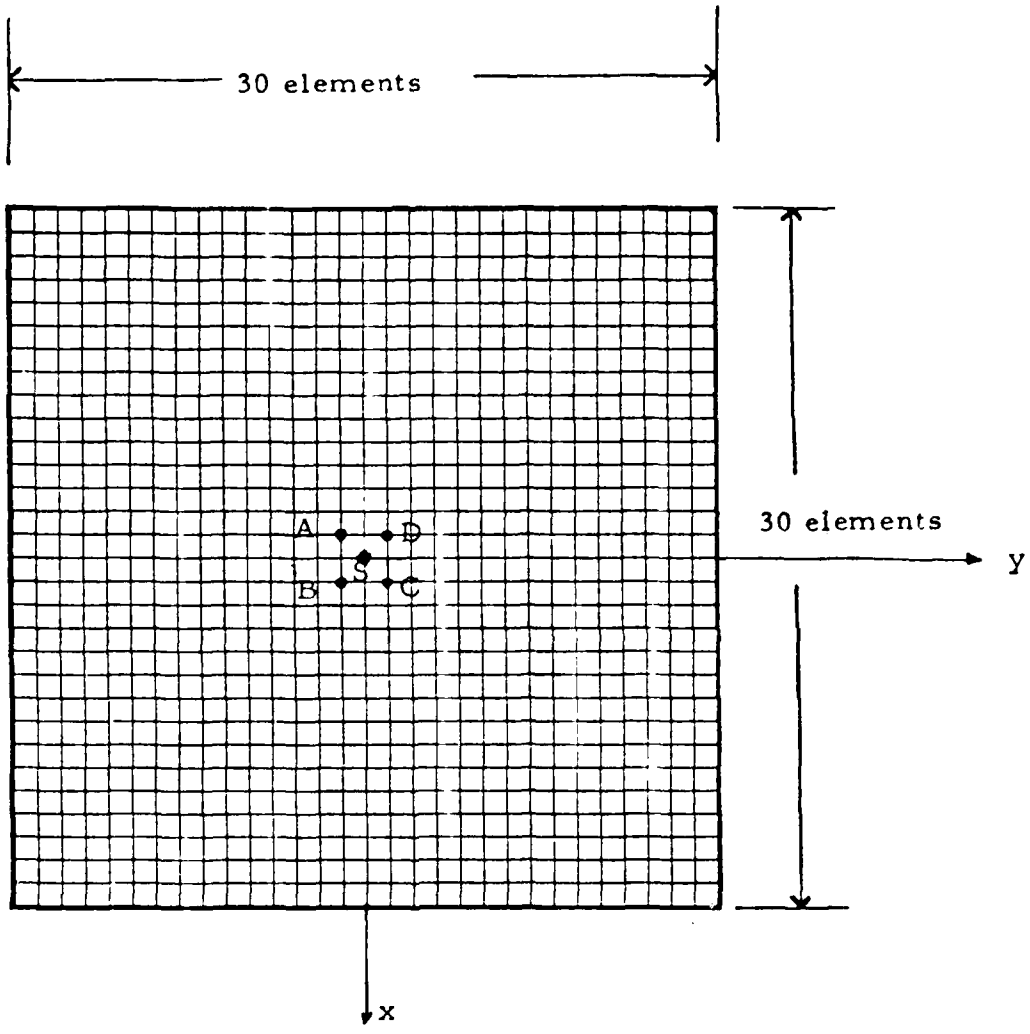

Figure 11. A 30x30 Finite Element Mesh of a Homogeneous Elastic Medium with V_p = 5,000 m/sec, V_s = 2,900 m/sec and ρ = 2.67 gm/cm^3. ($\Delta x = \Delta y = 100$ m)

(A) One Degree of Freedom SH-Wave Problem

(1) Concentrated Line Source

As we mentioned previously, this is the most natural way to apply an external source without making any effort. At Point S(Ø,Ø) in Figure 11, a forcing function $F_1(t)$ (Figure 7-A) is applied. Figures 12-A to 12-H are the displacement field at Ø.1 sec intervals. The cylindrically spreading wave propagation can be observed clearly.

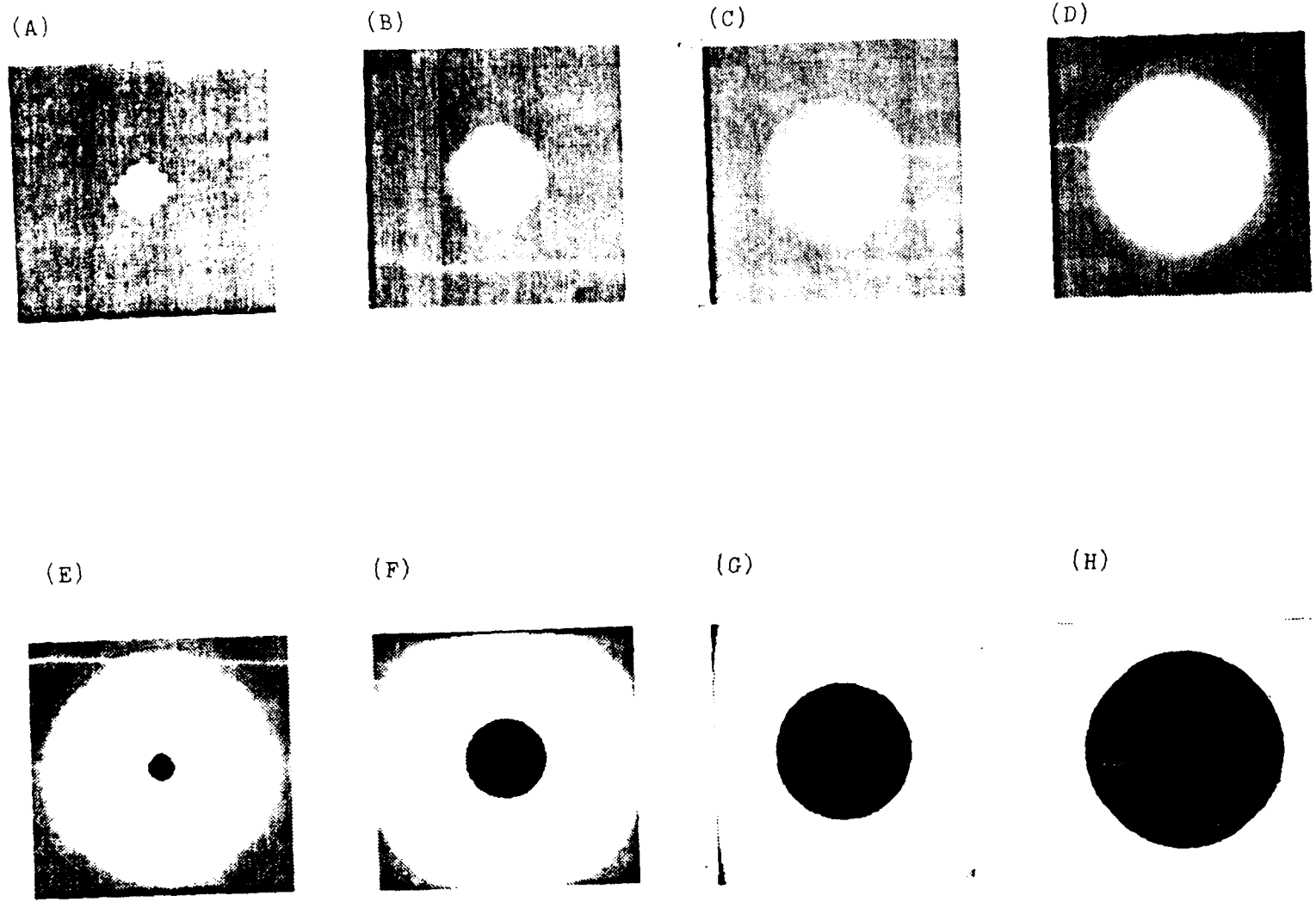

Figure 12. Snapshot View of Wave Pattern at 0.1 sec Interval After the Detonation of the Concentrated Line Source.

(ii) Concentrated Coupled Line Source

In order to simulate a coupled line source at point $S(\emptyset,\emptyset)$ of Figure 11, we set the points $S_1(\emptyset,+\emptyset)$, and $S_2(\emptyset,-\emptyset)$ occupying the same location as point S and apply the forcing function $F_1(t)$ to each individual point but in opposite directions as shown in Figure 13. In other words, the displacement fields are $w_1(\emptyset,+\emptyset,t)$ and $w_2(\emptyset,-\emptyset,t)$ at S_1 and S_2 respectively. At the source points in Figure 13, dot means outward from the plane of the paper, cross means inward towards the plane of the paper. Points A, B, C, and D are the nodal points surrounding point S in Figure 11. Figure 14-A to 14-H are the snapshots of the synthetic displacement field $w(x,y,t)$ at $\emptyset.1$ sec intervals showing the radiation pattern of a coupled source.

● Outward from the plane of the paper

X Inward towards the plane of the paper

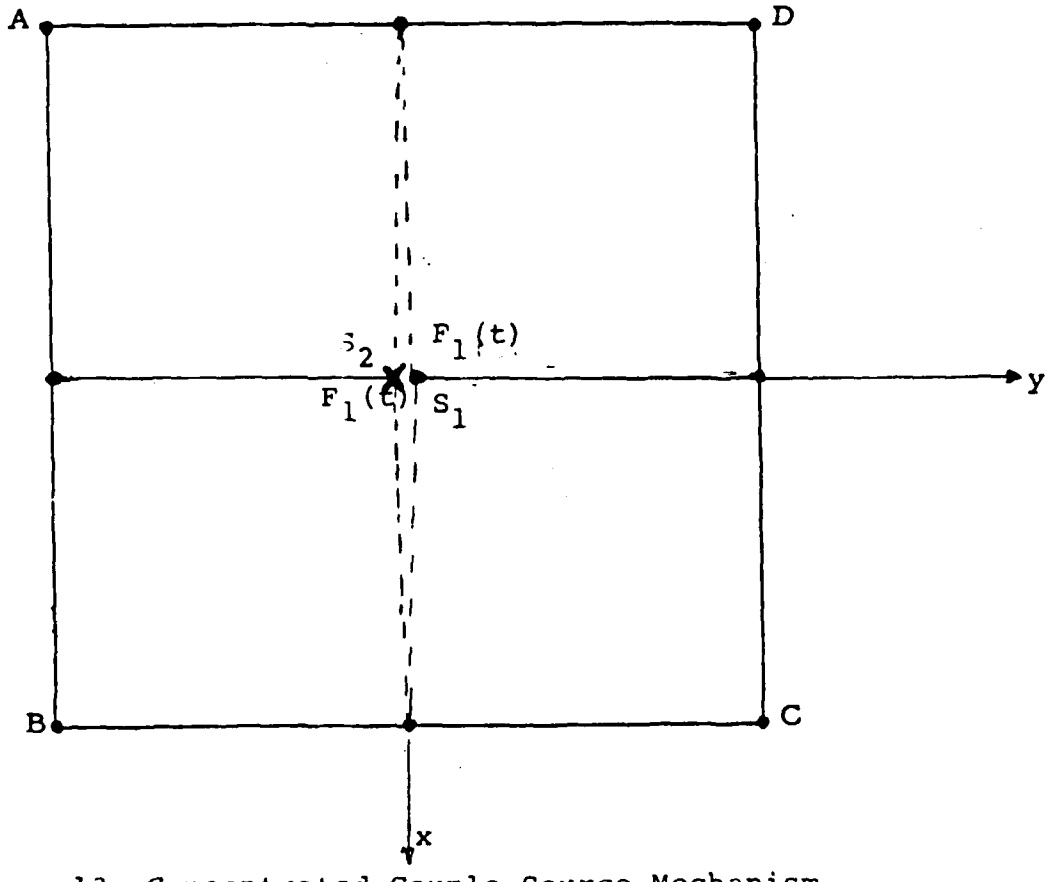

Figure 13. Concentrated Couple Source Mechanism for SH-Wave Case.

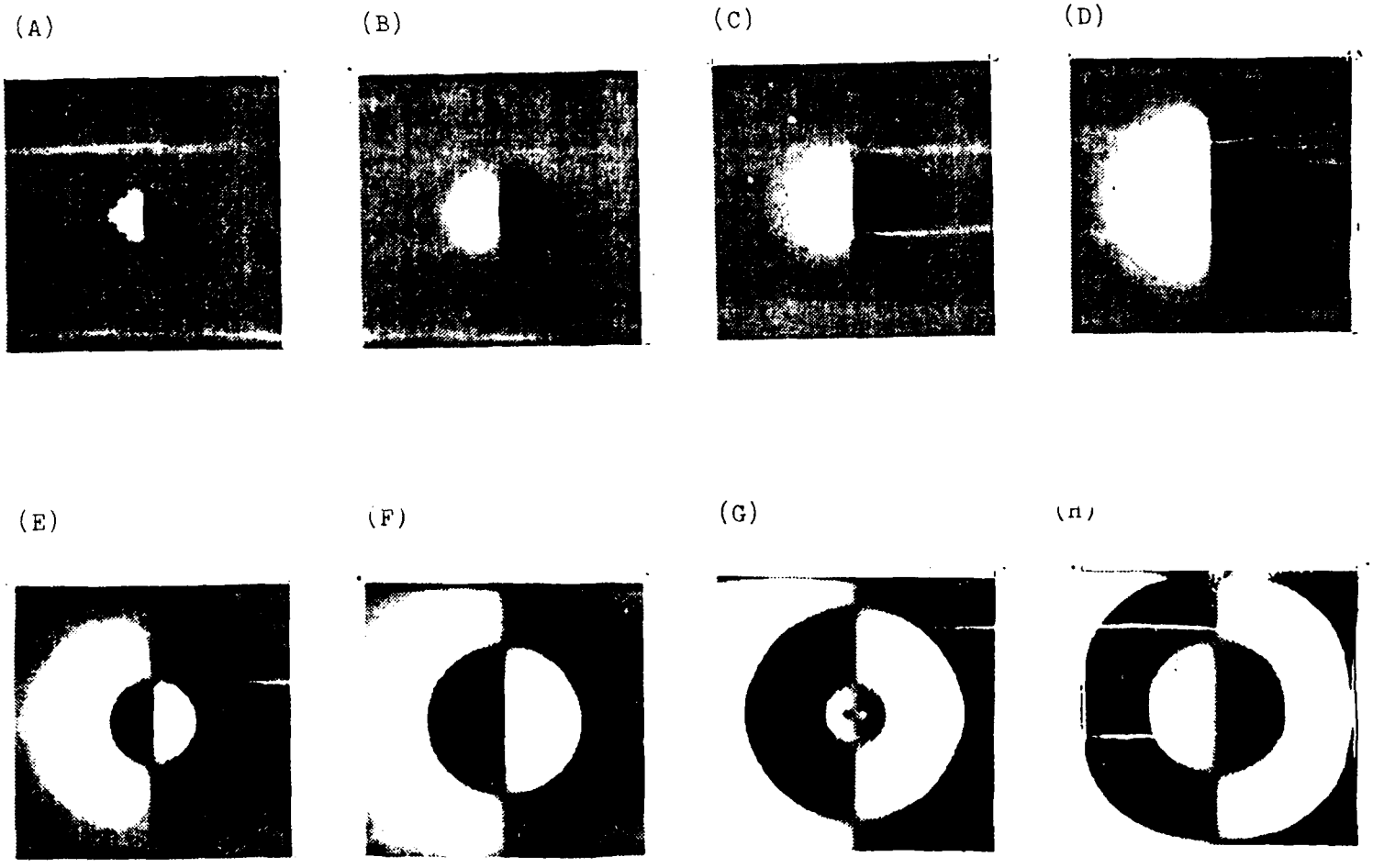

Figure 14. Snapshot View of Wave Pattern at 0.1 sec Interval After The Detonation of the Concentrated Couple Source.

1

(B) Two Degree of Freedom Elastic Wave Problem

(i) Directional Concentrated Line Source

For the elastic wave case, the most natural way of a source is the directional source. In Figure 15, a vertical line source $F_o(t)$ as shown in Figure 7-B is located at point S. Figures 16-A to 16-I are the snapshots of the absolute values of the displacement resultants. The time interval between snapshots is Ø.Ø575 sec.

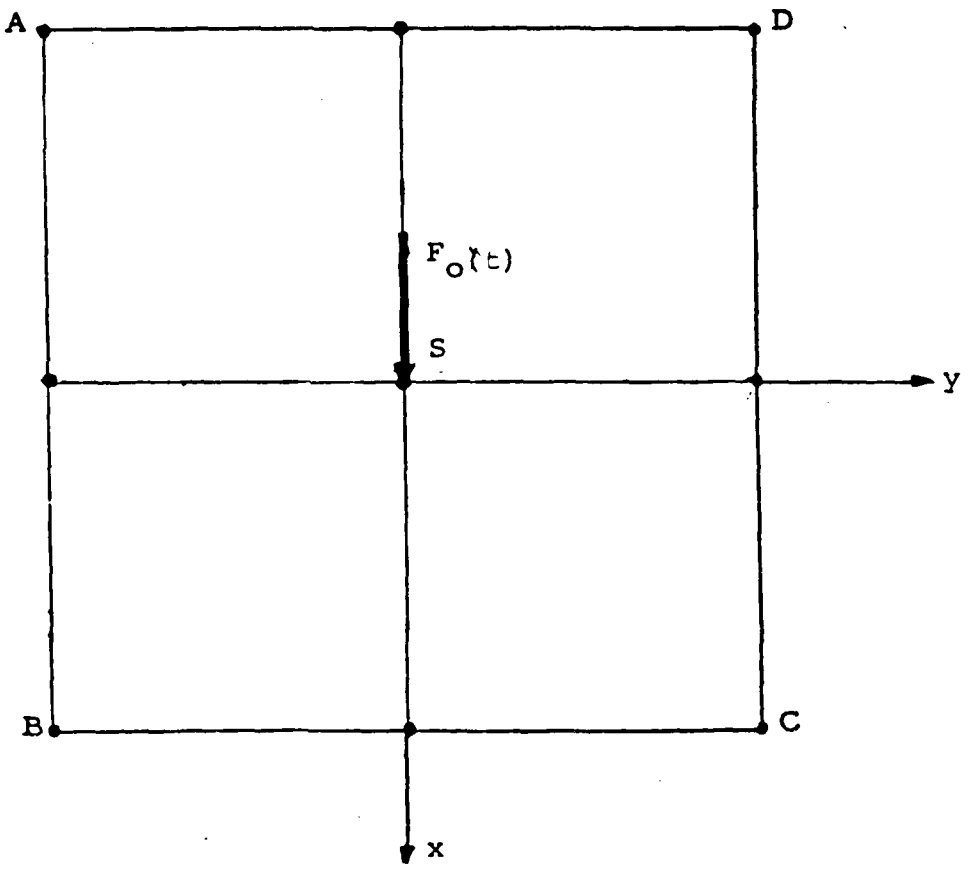

Figure 15. Directional Source for the Elastic Case.

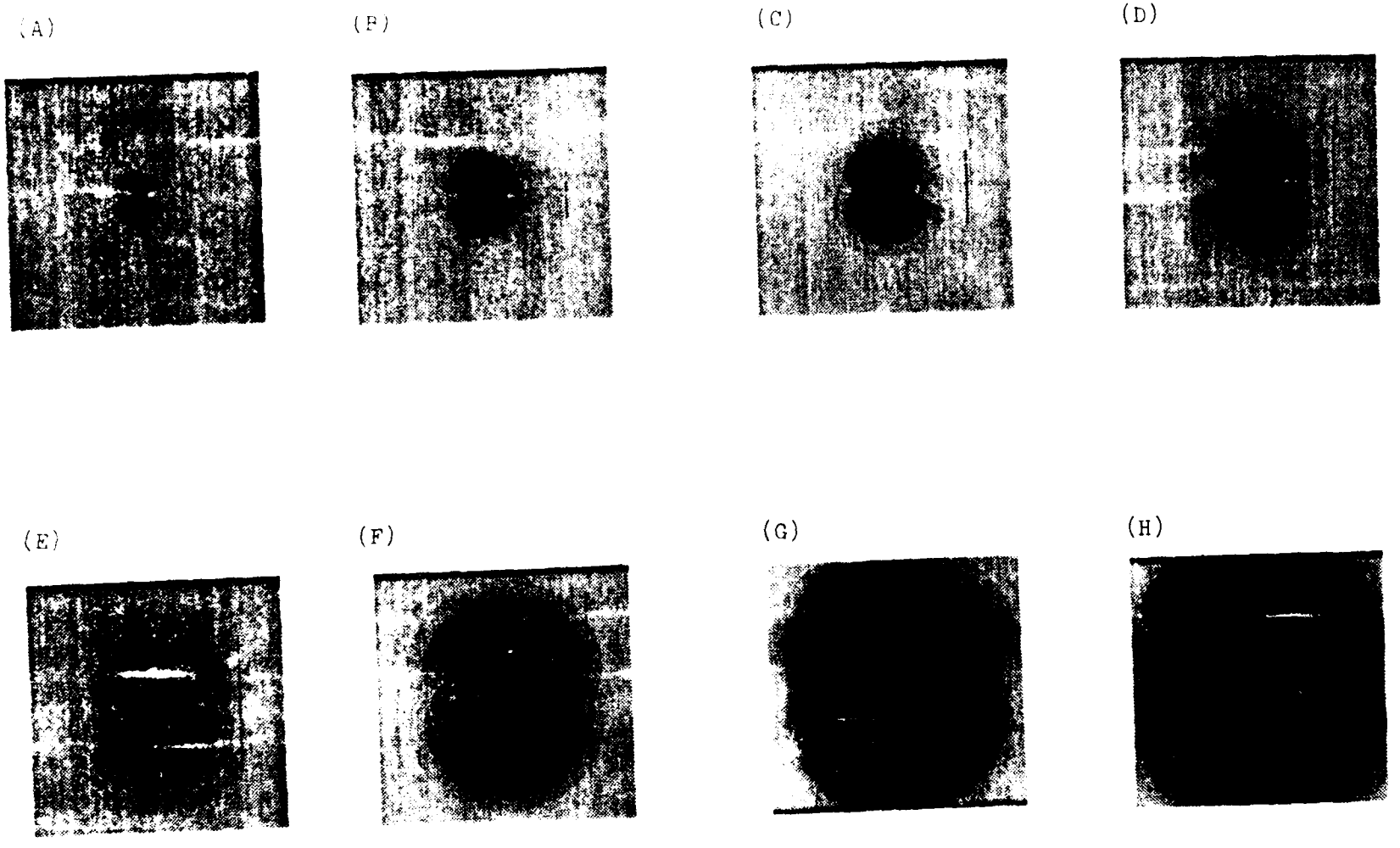

Figure 16, Snapshot View of Wave Pattern at 0.0575 sec Interval After the Detonation of the Directional Line Source.

(11) Concentrated Coupled Line Source

Figure 17 shows the mechanism of the coupled source for the elastic wave case. Points $S_1(\emptyset,+\emptyset)$ and $S_2(\emptyset,-\emptyset)$ occupy the same location and are subjected to a moment forcing function $F_o(t)$, with the same magnitude but opposite directions. The radiation patterns of the displacement magnitude are given in Figures 18-A to 18-H.

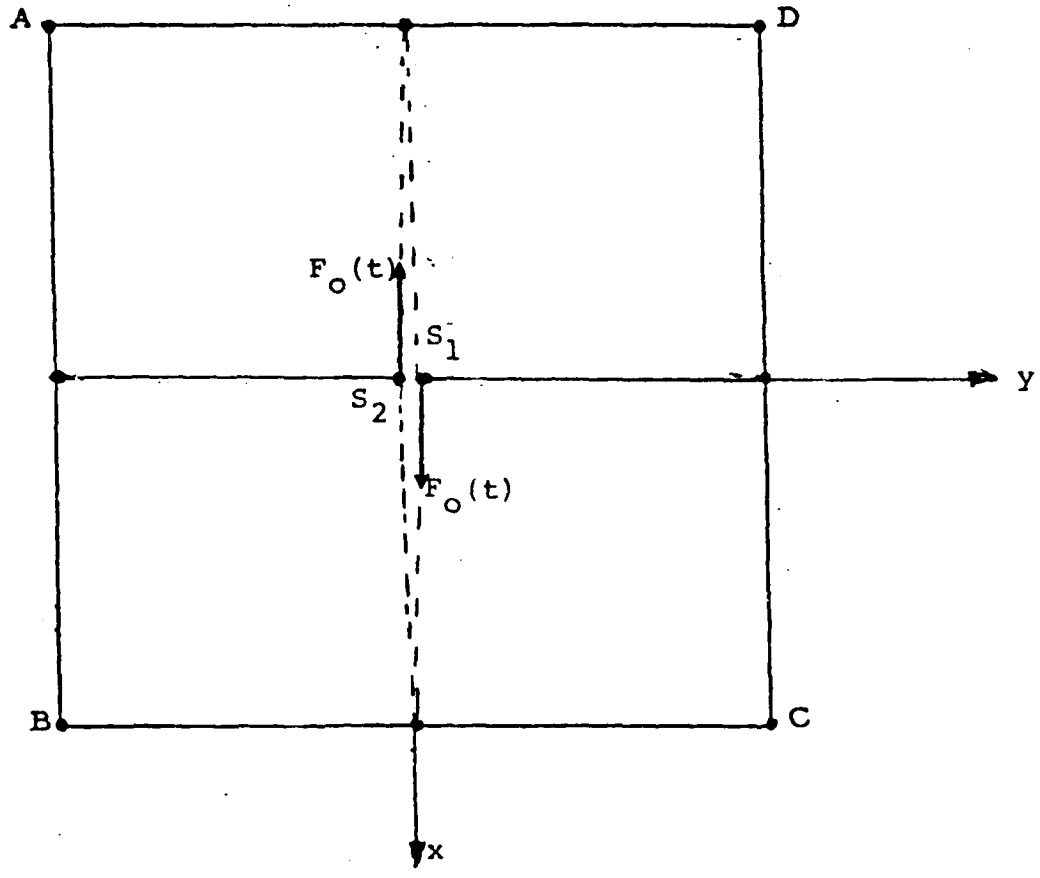

Figure 17. Concentrated Couple Source Mechanism for Elastic Case.

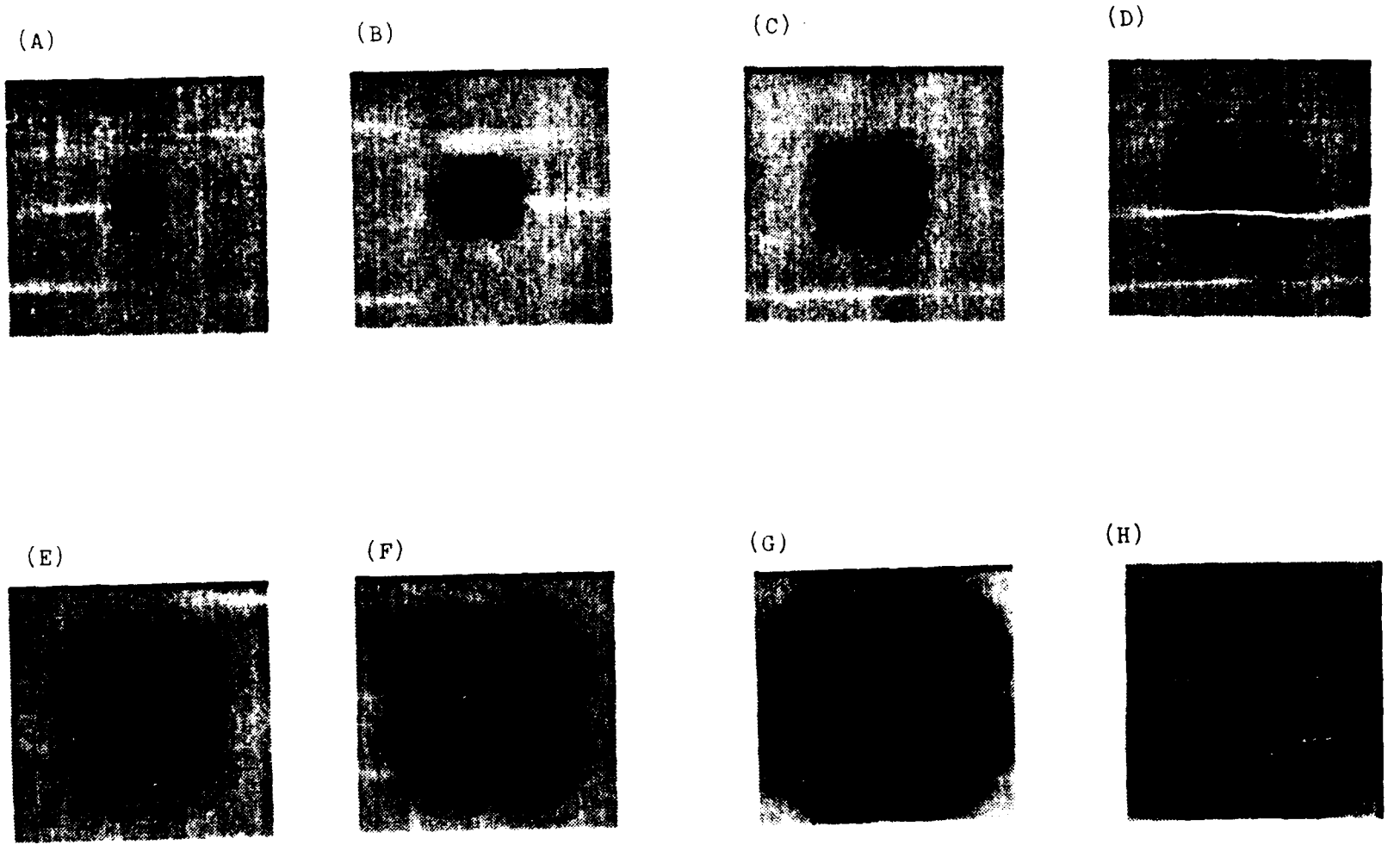

Figure 18. Snapshot View of Wave Pattern at 0.0575 sec Interval After the Dectonation of the Concentrated Couple Source.

(iii) Non-Directional Concentrated Line Source

In order to simulate a non-directional concentrated line source at point S(Ø,Ø) in Figure 11, we set the points $S_1(-Ø,+Ø)$,$S_2(+Ø,+Ø)$,$S_3(+Ø,-Ø)$, and $S_4(-Ø,-Ø)$ at the same location as point S and apply a forcing function $F_o(t)$ to each individual point in a manner shown in Figure 19. The cylindrically spreading radiation patterns of the displacement magnitude can be observed in Figure 2Ø-A to 2Ø-J.

In the preceding five cases, the non-reflecting boundaries technique are used on all four boundaries. Without using the non-reflecting bourdaries undesired reflections would start at the 15th time step, Ø.3 seconds for the SH-wave cases and Ø.1725 seconds for the elastic wave cases, after the detonation of the source.

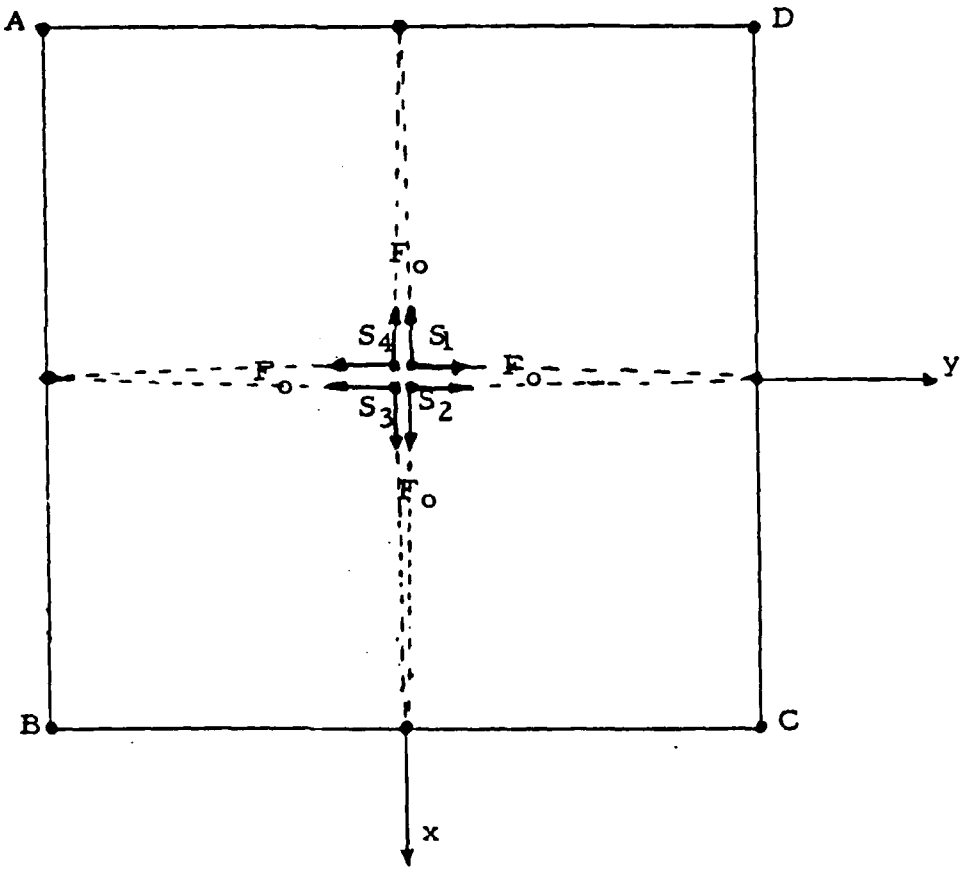

Figure 19. Non-directional Line Source Mechanism for Elastic Case.

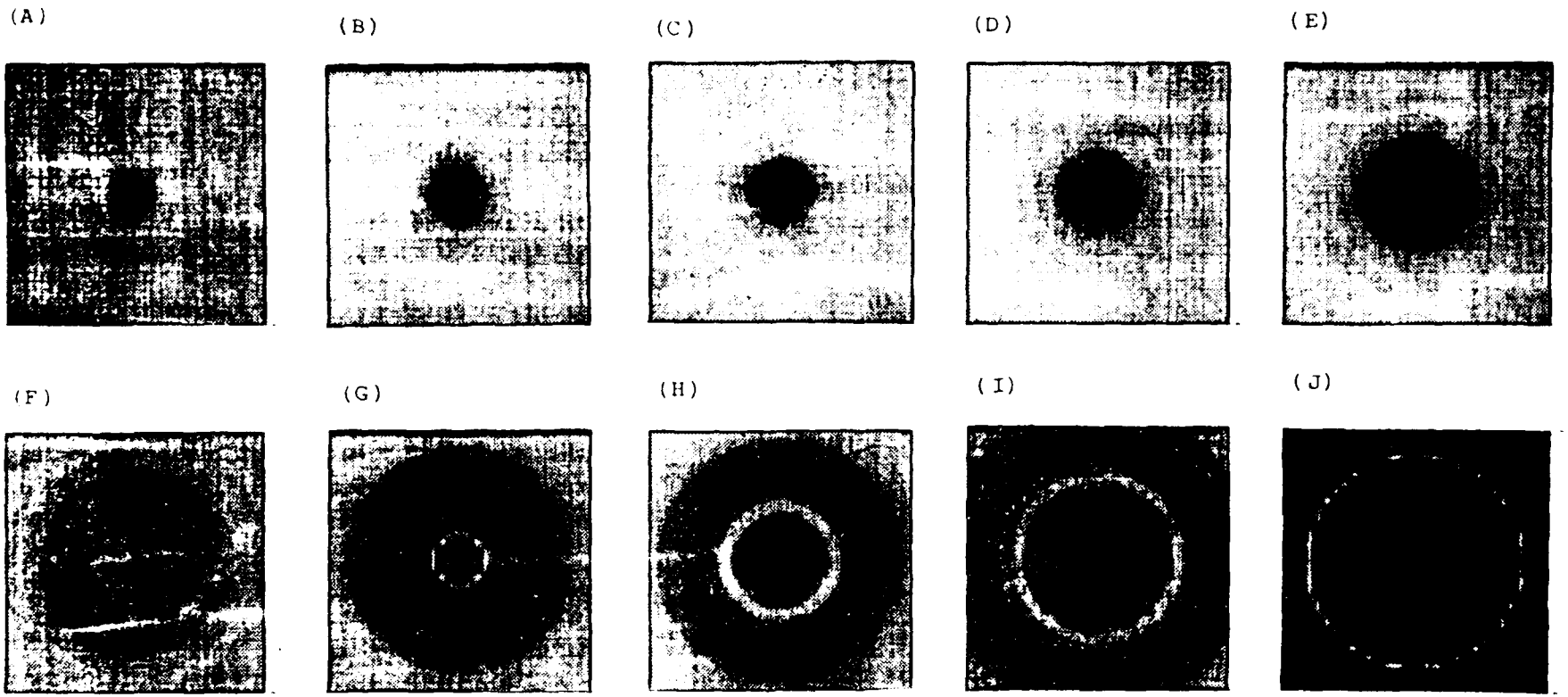

Figure 20. Snapshot View of Wave Pattern at 0.0575 sec Interval After the Detonation of the Concentrated Non-directional Point Source.

III. Modification of the Finite Element Codes

In the old version of our two-dimensional finite element codes, (SH-wave and Elastic Wave Cases), we used the 4-CST (Constant Strain Triangles) quadrilateral elements in order to avoid the space-grid skewness. The degree of freedom of the internal node, such as node 5 in Figure 21-A, is statically condensed. The degrees of freedom of such nodes do not appear in the global assemblage equations so that the storage during the computation is reduced considerably. The 4-CST formulation has been a very good approach to obtain solutions for static cases. However, in the algorithm of 4-CST for dynamic case, it was assumed that the internal condensed nodal points of each quadrilateral element were subjected to no inertial forces. In the present modified version of these codes, an average 2-CST algorithm is adopted. In Figure 21-B, a quadrilateral is composed of two triangles. Two distinct ways of subdividing the quadrilateral are given. Therefore, the assembled quadrilateral stiffness matrix can be obtained by linear interpolation without any internal condensation. Based on the averaging 2-CST formulation, a better approximation of the solutions can be obtained.

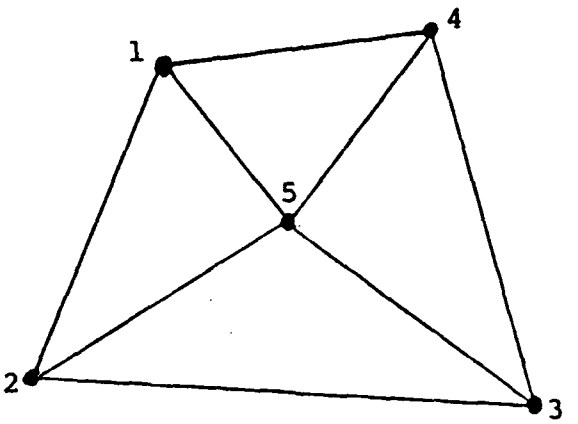

Figure 21-A. A 4-CST Quadralateral Element.

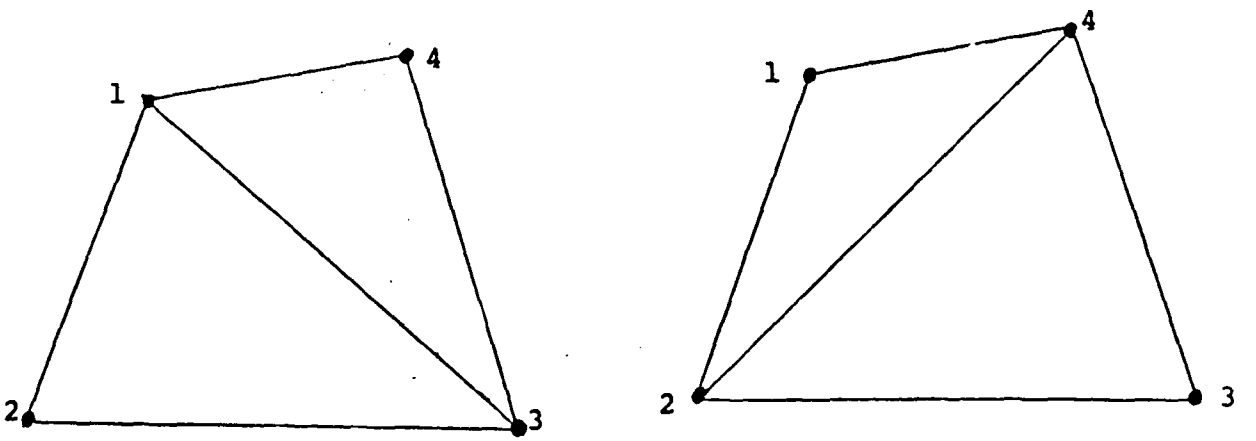

Figure 21-B. Two 2-CST Quadralateral Elements.

(B) Nodal-Point-Oriented Approach

In the old version of our two-dimensional finite element codes, the global stiffness matrix is obtained by the assemblage of the stiffness matrix of each individual quadralateral element for each time step in the time integration.

In the present modified version of the codes, the global matrix is assembled, only the non-zero stiffness matrix members are involved, for each nodal point before the compution of the time integration.

The advantages of the old codes are:

(i) The incore storage required is very little, only the products of the global stiffness matrix and displacements are stored.

(ii) Less mistakes can be made particularly for the source mechanism problems.

The advantages of the new codes are:

(i) The computing time is drastically reduced since local assemblages for each time step are avoided. The amount of the reduced time depends upon the size, the property of each individual problem. For a model of 40x40 elements, the computing time using the new version program is only 1/5 of that using the old version.

(ii) The disk storage for problems with irregular element meshes is the same as that of the problem with regular size element mesh.

In both versions, the 2-CST formulation and the effective excitation method are used. The restart back-up option is also valid for the new version codes.

FUTURE RESEARCH

The seismic velocity models for western alluvial basins have been studied extensively by Battis (1981). He derived a first-order model for a "typical" MX deployment alluvial basin with the features:

(i) The model basin is approximately 70 km in length with a width of 17 km,

(ii) Th maximum depth to bedrock within the valley is 2000 m.

(iii) The basin is enclosed by mountain ranges which parallel the major axis. These ranges are about 15 km wide with an average elevation of 750 m above the base floor.

(iv) The characteristic seismic velocity profile of the typical basin is as follows:

Layer	Thickness (meters)	Depth (meters)	V_p (km/sec)	V_s (km/sec)
1	10	0	0.9	0.3
2	115	10	1.6	0.55
3	75	125	2.0	0.8
4	200	200	2.25	1.1
5	400	400	6	1.5
6	450	800	3.0	1.75
7	(to basement)	1250	3.5	2.0
8	...	(basement)	5.0	2.9

(v) The typical basin in the deployment region is symmetric.

He further pointed out that the concept of a "typical" basin model is misleading. Each basin has its own significant variations from the typical one. In studying the seismic responses in alluvial basins, both the typical and variations on models must be considered.

Therefore, even a typical valley structure is a complex intermeshing of materials with high velocity gradients at least in two and probably all three dimensions.

In the past two years, our research emphasis of the present contract has been on the two-dimensional studies including preliminary basin modeling, source mechanism, and computer codes improvements in finite elements. In the coming year of the contract, the research, within the limit of the Aldridge PRIME 750 computer, would be:

(A) Extending the above two-dimensional studies to three dimensions.

(B) Simulating the two-dimensional alluvial basin models with as closely as possible to the first-order typical basin model derived by Battis or the models provided by the Air Force Geophysics Laboratory by finite element method with different type of sources.

ACKNOWLEDGEMENT

The authors wish to express their deep appreciation to Dr. Kurt Marfurt, for using his snapshots subroutine, to Messers. Ting-Fan Dai, Peter Pecholcs for their assistance in developing the plotting software.

The authors also want to thank Mr. James Battis and Dr. John Cipar of AFGL for their genuine coorperation and encouragement.

REFERENCES

1. Battis, J. C., "Seismic Velocity Models for Western Alluvial Basins" AFGL-TR-81-Ø139 Enviromental Research Papers, No.74Ø, May,1981, ADA1Ø8153

2. Kuo,J.T., and Y.C.Teng, Ground Response in Alluvial Basins Due to Seismic Disturbances, Scientific Report No.1, 1982, AFGL-TR-82-Ø279, ADA123683.

3. Kuo,J.T., and Y.C.Teng, Ground Response in Alluvial Basins Due to Seismic Disturbances, Scientific Report No.2, Air Force F19628-81-K-ØØ12, 1983.

END

DTIC

8-86